THE MERCURY 6 $^1P_1$ PHOTOSENSITIZED DECOMPOSITION OF CARBON DIOXIDE

A Dissertation

Presented to

the Faculty of the Department of Chemistry

College of Arts and Sciences

University of Houston

In Partial Fulfillment

of the Requirements for the Degree

Doctor of Philosophy

---

by

Calvin M. Wolff, B.S. Ch.E.

January 1968

DEDICATION

. . .a mi Betty, luz de mi vida, vino de mi sangre!

ACKNOWLEDGEMENT

I wish to acknowledge Dr. Richard Pertel, principal investigator of this research, for his patience, wisdom, and effort in guiding me through this research and my post-graduate education. This effort was supported by the Atomic Energy Commission under Contract No. AT-(40-1)-2844. I am indebted to Dr. William S. Gleason for fabricating the electrodeless arc used in this work. I wish to thank Professor M. R. Willcott for his patience and guidance in assisting me in the completion of the final requirements for my degree, and my committee for their guidance in the completion of my thesis. I thank my parents very much for the encouragement and support given me in completing the first nineteen years of my education, and likewise my wife for the latter.

THE MERCURY 6 $^1P_1$ PHOTOSENSITIZED DECOMPOSITION OF CARBON DIOXIDE

An Abstract of

A Dissertation

Presented to

the Faculty of the Department of Chemistry

College of Arts and Sciences

University of Houston

In Partial Fulfillment

of the Requirements for the Degree

Doctor of Philosophy

---

by

Calvin M. Wolff, B.S.

January 1968

ABSTRACT

A stable optical transmittance filter which removes 2537A radiation from a mercury arc while transmitting the 1849A radiation was developed and applied in performing the mercury 6 $^1P_1$ photosensitization of carbon dioxide. The products of this reaction were found to be carbon monoxide, mercuric oxide, and mercuric oxalate. The kinetics of the reaction indicate the formation of a complex between mercury 6 $^1P_1$ and carbon dioxide. The complex may either decay to HgO and CO or may decay to a metastable triplet state which combines with carbon dioxide to form the oxalate. The oxalate partially decomposes photolytically during the reaction yielding the reactants carbon dioxide and mercury.

TABLE OF CONTENTS

TABLE OF CONTENTS CONTINUED

TABLE OF CONTENTS CONTINUED

LIST OF FIGURES

LIST OF FIGURES CONTINUED

LIST OF TABLES

I.

INTRODUCTION

INTRODUCTION

This work is a study of the decomposition of carbon dioxide by photosensitization with mercury 6 $^1P_1$ atoms. In this work, photosensitization is the transfer of all or some of the energy of a photolytically exited atom or molecule to another, and usually different kind, of molecule. In this case, the photolytically excited species is the mercury atom.

The Principles of Resonance Radiation and Excited Atoms

An excellent reference work on this subject was written by Mitchell and Zemansky (1), to which all the aspects of resonance radiation and excited atoms are discussed in detail and are thoroughly referenced.

There are two principle modes of photolytic excitation of mercury atoms. One mode involves the absorption of a photon of approximately 2537Å wavelength, causing the mercury to rise from its ground state to its first excited triplet state:

$$Hg6\ ^1S_o + h\nu\ (2537A) \rightarrow Hg6\ ^3P_1$$

The other excitation mode involves the absorption of a photon of approximately 1849A wavelength, causing the mercury atom to rise from its ground state to its first excited singlet state:

$$Hg6\ ^1S_o + h\nu\ (1849A) \rightarrow Hg6\ ^1P_1$$

The probability of a mercury atom absorbing a photon of wavelength λ to perform an electronic transition is expressed by the extinction coefficient, k_λ, of mercury. The physical significance of the extinction coefficient is expressed by its mathematical relationship to the efficiency of absorption by mercury atoms of radiation at wavelength λ:

$$\frac{I_\lambda^o - I_\lambda \text{Absorbed}}{I_\lambda^o} = e^{-k_\lambda l N}$$

where N = concentration of mercury atoms

l = optical path of mercury atoms

e = base of natural logarithm

I_λ Absorbed = intensity of radiation passing through λ that is absorbed

I_λ^o = intensity of radiation incident to l.

Note that k_λ represents a cross section of the mercury atom, making "collision" of a photon at wavelength λ and the mercury atom analogous to the collision of molecules in a gas; that is, the greater the cross sections, the greater the probability of collision. Thus k_{2537A} would be a measure of the rate of conversion of Hg6 ^1S_o atoms to Hg6 $^1P_1$ atoms in a flux of 2537A photons.

An excited mercury atom in a foreign gas may either decay naturally to its ground state, emitting a photon of the same wavelength it absorbed, and having a mean lifetime of τ, or it may collide with a

foreign gas molecule. In the latter case the excited Hg atom either transfers its energy of excitation to the foreign gas molecule and returns to its ground state or be caused to prematurely decay to its ground state, emitting a photon. The first case is known as resonance; that is, oscillating between two electronic states by receiving and emitting the same frequency of energy. The second case, where the energy of excitation is transferred to the foreign gas molecule, has been defined above and is known as photosensitization.

Phenomena which effect the lifetimes of excited atoms also effect the "breadth" of the respective emission line. The "breadth" of a mercury emission line is the half width in frequency or wavelength units of this line in its emission spectrum. It is related to the lifetime of the excited state, τ, by the Heisenberg uncertainty principle:

$$\Delta E \Delta t = h/2\pi$$

where h = Planck's constant

ΔE = uncertainty in the energy of the transition

Δt = uncertainty in the transition time

Since

$$\Delta E = \frac{c h \Delta \lambda}{\lambda^2} \text{ and } \Delta t = \tau, \text{ c = speed of light,}$$

then the width of the natural emission line, $\Delta\lambda$, is proportional to $\frac{\lambda^2}{2\pi\tau c}$.

Consider the case in which the excited mercury atom is caused to prematurely radiatively decay upon collision with a foreign gas molecule. Ordinarily radiative decay is governed by the natural lifetime of the excited mercury atom, τ, such that the rate of decay of excited atoms, say $Hg6\ ^1P_1$ atoms, is equal to

$$(1/\tau)(Hg6\ ^1P_1).$$

The effect of collision and premature radiative decay is then to shorten the lifetime of the excited state, thereby increasing the breath, or broadening the emission line. Since this broadening increases with the number of collisions of the foreign gas, i.e., its pressure, this phenomenon is known as pressure broadening.

The wavelength of emission lines, as viewed externally from the emitting atoms, is subject to displacement in apparent wavelengths due to the motion of the emitting atoms. This is more commonly known as the Doppler effect, and the broadening of the emission lines caused by this effect is known as Doppler broadening.

The presence of foreign gas molecules, and also high concentrations of mercury atoms, gives rise to line broadening in absorption. This type of broadening is known as Lorentz broadening. The effect of Lorentz broadening is to broaden the absorption line, shift its peak wavelength and cause the shape of the line to be asymmetric. Thus a sufficient pressure of foreign gas molecules may cause an increase in the efficiency of photosensitized reactions.

The Details of Photolytic Excitation of Mercury

The use of a single absorption coefficient of mercury for its own rasonance radiation is an oversimplification. There are several parameters governing the probability of "resonance" excitation of mercury. First, the spectral "line" corresponding to a mercury-transition or absorption is actually a composite of several "hyperfine lines", due to perturbations of the energy of the transition caused by the interaction of the nuclear spin of the atom with the electronic orbitals, just as multiplet spectral lines evolve from interaction of the electronic spins and orbitals. In the case of a net nuclear spin of zero, the hyperfine structure will consist of only one line, as in the case of the even numbered isotopes. In the case of the odd numbered isotopes, however, the hyperfine structure will consist of several lines, since the corresponding nuclear spins are not zero. The hyperfine structure of natural mercury for the $Hg6\ ^1P_1 \rightarrow Hg6\ ^1S_o$ transition, consisting of a mixing of the hyperfine structure of its component isotopes, as a function of their natural abundance, is depicted in Figure 1. Each hyperfine line is effected by natural, Doppler, and pressure broadening and other types of broadening.

These spectra may be either emission or absorption spectra. If they are emission spectra, then let the ordinate be defined as spectral irradiance, J_λ:

$$J_\lambda = \frac{dI_\lambda}{d\lambda}$$

FIGURE 1

HYPERFINE STRUCTURE OF NATURAL MERCURY LINE AT 2537Å

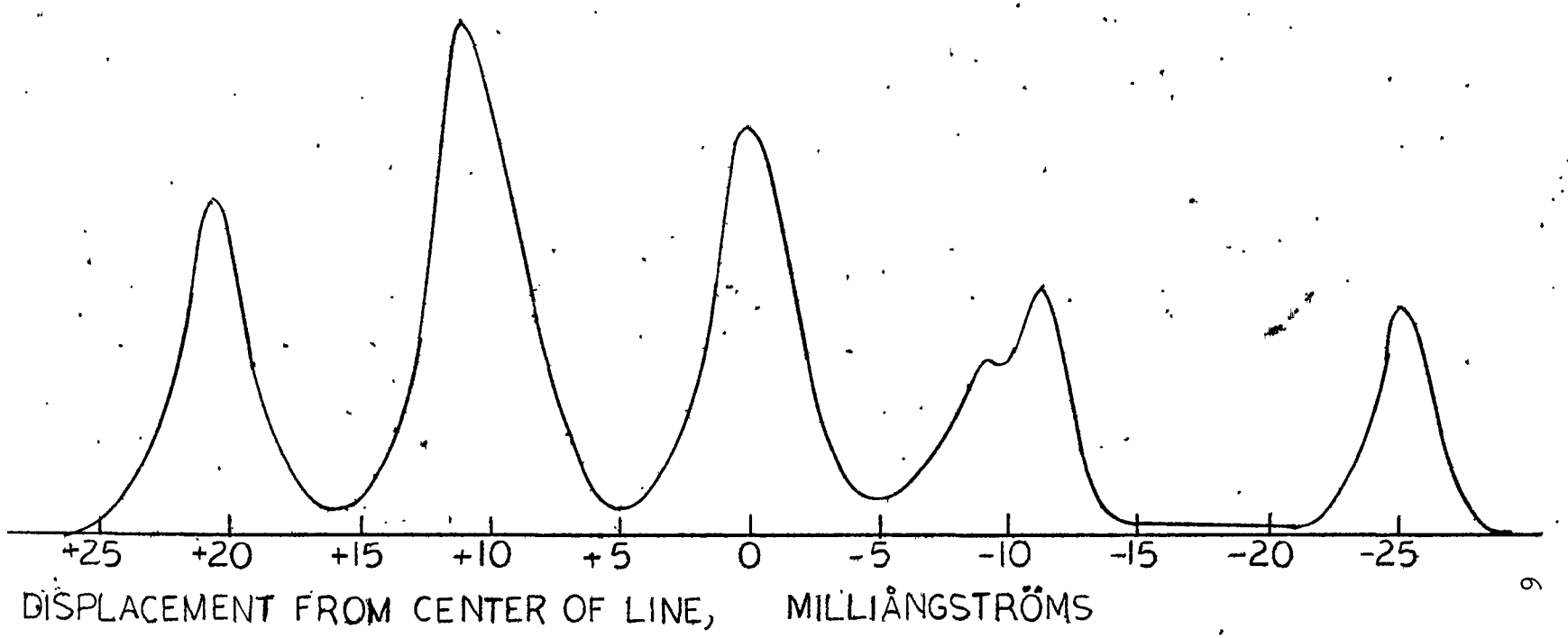

where I_λ = irradiance at wavelength λ, in units of quanta cm^{-2} sec^{-1}. If these spectra are absorption spectra, then let the ordinate be defined as the extinction coefficient, k_λ, at wavelength λ, such that the absorption of mercury atoms at wavelength λ for any source is $1 = e^{-k\lambda lN}$

$$\text{Quanta absorbed} = \int_o^\infty J_\lambda d\lambda - \int_o^\infty J_\lambda e^{-k\lambda lN} d\lambda$$

Qualitatively, this ratio can be visualized by superimposing the emission curve of the source on the absorption curve of the receiver. If it is desired to have a single value to represent the absorption or transmission efficiency of a specific case, then the extinction coefficient defined earlier can be applied:

$$\text{Quanta transmitted} = e^{-K\lambda lN} = \int_o^\infty J_\lambda e^{-k_\lambda lN} d\lambda$$

In the research described in this thesis, the same (natural) mercury (arc) emission source and the same composition (natural) of mercury vapor was employed in all quantitative experiments, and the quantity $e^{-K\lambda lN}$ was measured experimentally for both resonance lines of mercury, so that knowledge of k_λ and J_λ was not necessary to this research effort.

The Details of Photosensitization by Excited Mercury Atoms

Once the mercury has become excited by the processes detailed above, it may interact with another molecule before natural decay.

The probability of this interaction is proportional to the populations of excited mercury atoms and to the affinity of the two species for interaction. This may be expressed kinetically, for Hg6 $^1P_1$ atoms, as interaction rate = k $(Hg6^1P_1)(M)$, where $(Hg6^1P_1)$ and (M) are the concentrations of Hg6 $^1P_1$ atoms and the interacting species molecules M, respectively, and k is proportional to the quenching efficiency between $Hg6^1P_1$ atoms and M molecules and to the kinetic motion of the gas molecules.

The factor k can be expressed in more detail by:

$$k = \sigma^2[8\pi RT\ (\frac{1}{M_{Hg}} + \frac{1}{M_x})]^{1/2}$$

where R = gas constant

T = temperature

M_x = molecular weight of species x

σ^2 = quenching cross section

The term in brackets expresses the kinetic dependence of the interaction and σ^2 represents the quenching efficiency for the interaction of Hg6 $^1P_1$ and M. The term quenching cross section expresses well the physical significance of σ^2. It is a cross section analagous to, but not the same as, the collision cross section of colliding molecules in a gas. It is the cross section term applied to the kinetic suffix (in brackets) which governs the quenching of the excitation energy of the excited atom, in this case Hg6 $^1P_1$, by the molecule M. Various quenching cross sections are listed in Table I.

TABLE I

QUENCHING CROSS SECTIONS OF VARIOUS MOLECULES FOR

Hg6 $^3P_1$ and Hg6 $^1P_1$ ATOMS

Molecule	σ^2 for Hg6 $^3P_1$, A^2	σ^2 for Hg6 $^1P_1$, A^2
H_2	8.60 (1)	No reliable
H_2O	1.43 (1)	values have
NO	35.3 (1)	thus far been
CO_2	3.54 (1)	determined.
NH_3	4.20 (1)	
O_2	19.9 (1)	
Benzene	60 (1)	

It should be mentioned that "quenching" does not only mean sending the excited atom to its ground state. The atom, Hg6 $^3P_1$ for example, may be "quenched" just to its metastable state, Hg6 ^3P_o, which involves the transfer of only 0.218 electron volts, compared to 4.86 electron volts for quenching it to Hg6 ^1S_o.

Both processes, quenching and natural decay, should be considered collectively as competing processes. Excited atoms, in this case Hg6 $^1P_1$, are formed according to

$$Hg6\ ^1S_1 + h\nu\ (1849A) \rightarrow Hg6\ ^1P_1,\ \text{rate} = I_{1849}\ (\text{assuming } e^{-kNl} < 0.01).$$

The excited atoms are consumed by decay and by quenching (photosensitization), respectively, as follows:

$$Hg6\ ^1P_1 \rightarrow Hg6\ ^1S_o + h\nu\ (1849A)\ \text{rate} = 1/\tau(Hg6\ ^1P_1)$$

$$Hg6\ ^1P_1 + M \rightarrow Hg6\ ^1S_o + M_{excited}$$

$$Hg6\ ^1P_1 + M \rightarrow (Hg - M)_{excited} \qquad \text{rates} = k(Hg6\ ^1P_1)(M)$$

Thus a steady state treatment of the processes, with respect to $Hg6\ ^1P_1$, would lead to:

$$\frac{d(Hg6\ ^1P_1)}{dt} = 0 = I_o - \frac{1}{\tau}(Hg6\ ^1P_1) + k(Hg6\ ^1P_1)(M). \quad (Hg6\ ^1P_1) = \frac{I_o}{1/\tau + k(M)}.$$

If $(M)_{excited}$ or $(Hg - M)_{excited}$ spontaneously decomposed leaving products other than Hg or M, the rate of appearance of the products would be, by steady state considerations,

$$\frac{1}{Q} = \frac{kI_o(M)}{[1/\tau + k(M)]}$$

where Q = inverse of product appearance rate.

It is seen that

$$Q = \frac{[1/\tau + k(M)]}{kI_o(M)} = \text{constant} \cdot \left[\frac{1}{\tau k(M)} + 1\right]$$

and therefore the quantities $1/\tau$ and $k(M)$ are competitive in determining the rate of photosensitization product formation.

The value k may be calculated, and thus σ^2 of M for Hg6 $^1P_1$, by drawing a plot of relative Q vs. $(M)^{-1}$. The value of $(M)^{-1}$ corresponding to twice the value of Q at the intercept [$(M)^{-1}$ approaches zero] is substituted into the equation $k(M)\tau = 1$, which is true at that point, and the value $k = \frac{1}{\tau M}$ is determined. The values of τ for the Hg6 $^1P_1 \rightarrow$ Hg6 ^1S_o and Hg6 $^3P_1 \rightarrow$ Hg6 ^1S_o have been experimentally determined to be approximately 10^{-9} sec and 10^{-7} sec (1), respectively.

It is the object of this thesis to determine products formed by the reaction of carbon dioxide with Hg6 $^1P_1$ atoms, as well as mechanisms and intermediates involved in the formation of these products. Previous work has been done on this subject and is summarized in the following section.

The History of the Experiments on the Hg6 $^1P_1$-CO_2 Reaction

The first Hg6 $^1P_1$ photosensitized reactions were accidentally performed during photolysis reactions using mercury lamps in systems containing mercury (2,3,4). The unrecognized photosensitization gave results which were always the same. Moist CO_2 gave very low yields compared to dry CO_2. The explanation given at the time involved catalysis by H_2O. Actually, the water vapor quenched the Hg6 $^1P_1$ atoms at a much higher rate than the CO_2 atoms did. Chapman, Chadwick, and Ramsbottom (2) noted that in the dry CO_2 pressure range studied, the yields were independent of pressure, which can now

be explained as caused by the nearly complete quenching of the Hg6 $^1P_1$ atoms by CO_2 in that pressure region (above 36 torr). All of the early researchers found that when carbon dioxide was decomposed a yellow film of mercuric oxide was present. Coehn and May (5) found that CO_2 dried with concentrated sulfuric acid and phosphorous pentoxide did not decompose upon irradiation, but when mercury droplets were added to increase the sensitivity of oxygen detection by yellow film formation, the same carbon dioxide decomposed very efficiently. From these results they concluded that carbon dioxide was decomposed by Hg6 $^3P_1$ atoms formed by the 2537A component of the irradiation. Cline and Forbes (6) later proved that photosensitization was the cause of the CO_2 decomposition but it was due to the Hg6 $^1P_1$ atoms from the 1849A component of mercury arc rather than Hg6 $^3P_1$ atoms. They reported the products of the reaction to be only carbon monoxide in the gas phase and mercuric oxide as a yellow film. Cline and Forbes also photolyzed carbon dioxide and found it to have a very low quantum yield, 0.0029 at 23.5 torr, as compared to the quantum yield of photosensitization, which they reported to be 0.8. They also reported that the yield of decomposition by 2537A radiation in the absence of 1849A radiation was not detectable.

Later, Strauss and Gunning (7) re-examined the photosensitized decomposition of CO_2 with Hg6 $^3P_1$ and Hg6 ^3P_o atoms. They verified that the yield was very low, in the range of 0.01 torr. However, decomposition to carbon monoxide as the only gas phase product and

mercuric oxide as a yellow film did take place. They attributed the formation of mercuric oxide to the scavenging of oxygen atoms by mercury. The reaction was found to be proportional to the 1.8 power of the 2537A intensity. The yield increased when nitrogen molecules were present, and the addition of 4047A mercury arc radiation enhanced the yield even more in the presence of nitrogen, but did not have an effect without the nitrogen. They also found that the rate decreased as the CO_2 pressure became very large. Their explanation is plausible and quite interesting. The carbon dioxide molecules are vibrationally excited by their first collision with Hg6 $^3P_1$ or Hg6 ^3P_o:

$$Hg6\ ^3P_1 \text{ or } Hg6\ ^3P_o + CO_2 \rightarrow Hg6\ ^1S_o + CO_2^*$$

The collision of a vibrationally excited CO_2 molecule with another excited mercury atom gives CO_2 sufficient vibrational energy to undergo decomposition:

$$Hg6\ ^3P_1 \text{ or } Hg6\ ^3P_o + CO_2^* \rightarrow Hg6\ ^1S_1 + O + CO$$

The addition of nitrogen produces more metastable mercury atoms, Hg6 ^3P_o, which are longer lived and therefore have more probability of decomposing CO_2:

$$Hg6\ ^3P_1 + N_2 \rightarrow Hg6\ ^3P_o + N_2\ (0.218\ ev)$$

Higher carbon dioxide pressures have a greater probability of deactivating vibrationally excited CO_2 molecules:

$$CO_2^* + CO_2 \rightarrow 2CO_2 + \text{heat}$$

Addition of 4047A mercury radiation increases the yield only in the presence of nitrogen, by the formation of Hg7 $^1P_1$ atoms which can decompose CO_2 with a single collision:

$$Hg6\ ^3P_o + h\nu\ (4047A) \rightarrow Hg7\ ^1P_1$$

$$Hg7\ ^1P_1 + CO_2 \rightarrow Hg + O + CO$$

$$\text{or} \rightarrow HgO + CO$$

Mori (8) studied the Hg6 $^1P_1$ photosensitized decomposition of carbon dioxide in a very thorough and quantitative fashion. He did not isolate Hg6 $^1P_1$ atoms from Hg6 $^3P_1$ atoms since he also established that the Hg6 $^3P_1$ decomposition of CO_2, although evident, was negligible compared to that by Hg6 $^1P_1$ atoms. Mori found that carbon monoxide was the only gas phase product, and that a yellow film appeared on the reactor which he reported to be mercuric oxide. It is of interest to note here that he performed the reaction in the absence of mercury atoms; that is, a photolysis at 1849A, and found that molecular oxygen was produced. He found the ratio of CO to O_2 produced by photolysis to be about five to one, and attributed the deficiency in O_2 to wall adsorption of oxygen. Analyses of the products of CO_2 photolysis deeper in the vacuum ultraviolet (9) (e.g., xenon resonance lines have also reported oxygen atoms produced), and deficient with respect to the CO formed. Mori reported, as did Cline and Forbes, that the quantum yield of CO_2 photolysis at 1849A was very low, due to the very weak absorption of 1849A radiation by carbon dioxide. He deduced from

his data that the quenching cross section of CO_2 for Hg6 $^1P_1$ atoms was 320A or 64A, depending whether the natural lifetime of Hg6 $^1P_1$ atoms was 0.3×10^{-9} seconds or 1.6×10^{-9} seconds, respectively. McGilvary and Winkler (10) reported that the quenching cross section of carbon dioxide for Hg6 $^3P_1$ atom was 2.48A.[2] Mori attributed the much greater quenching of Hg6 $^1P_1$ atoms to the induced dipole-dipole interaction between mercury and carbon dioxide.

Mori postulated that the charge transfer interaction is quite favored in the case of Hg6 $^1P_1$ atoms, at least with respect to Hg6 $^3P_1$ atoms, since less energy is required for the transfer of an Hg6 $^1P_1$ electron to CO_2 than in the transfer of an Hg6 $^3P_1$ atom to a carbon dioxide molecule. This charge transfer concept brings the discussion back into the realm of pure chemistry. Back in 1868, Drechsel (11) discovered that dry carbon dioxide would combine with sodium and potassium vapor at high temperatures (400°C) and over silica dust to form their respective oxalates. These reactions were studied in detail by Lemarchands and Roman (12) who concluded, from thermochemical reasoning, that the reaction was a direct fixation of carbon dioxide by the alkali metals:

$$2M + 2CO_2 \rightarrow M_2C_2O_4,$$

rather than proceeding by first reducing the carbon dioxide.

$$2M + CO_2 \rightarrow M_2O + CO.$$

This "direct fixation" of carbon dioxide by alkali atoms might well be ascribed to transfer of the electron of the alkali atom to the carbon dioxide molecule, forming a charge transfer complex, M-O-C=O, which decomposes forming the oxalate:

$$2M\text{-}O\text{-}C{=}O \rightarrow \begin{matrix} M\text{-}O\text{-}C{=}O \\ | \\ M\text{-}O\text{-}C{=}O \end{matrix}$$

The probability of charge transfer complex formation is a function of the ionization potential of the metal and the electron affinity of the carbon dioxide. The ionization potential of Hg6 $^1P_1$ atoms is less than that of potassium or sodium, so that if carbon dioxide is truly an acceptor in forming charge transfer complexes leading to oxalate formation, mercury 6 $^1P_1$ atoms can undergo this reaction with greater ease than other (Na, K) donors that have already been shown to perform it.

Wolff and Pertel (13), in a preliminary publication on the research described in this thesis, reported to have found an oxalate of mercury in the photosensitized decomposition of carbon dioxide by Hg6 $^1P_1$ atoms and Hg6 $^3P_1$ atoms. They found that the oxalate did not occur when 2537A radiation was allowed in the reactor, presumably because this radiation decomposed the oxalate as fast as it was formed. They also reported that HgO and CO were the only other products, and that the reaction was wall dependent due to its marked decrease in rate with decrease in mercury vapor pressure. Later experiments in this research, and re-examination of the original data,

however, tend to indicate that the reaction is not wall dependent. The decrease in rate of decomposition is attributed to the mercury vapor being consumed by the reaction faster than it could be replaced when the mercury vapor pressure was very low.

It is apparent in the light of the previous work that some type of preliminary complex is formed in the Hg6 $^1P_1$-CO_2 reaction. The appearance of oxalate and the formation of HgO and CO as the only products of decomposition require the existence of such a complex. It is the object of this thesis, then, to establish the experimental conditions for conducting the Hg6 $^1P_1$-CO_2 reaction, and to elucidate the role of this complex in generating the reaction products.

The Properties of Carbon Dioxide

Before the execution of this research is discussed, it is necessary that the properties of the quenching gas, carbon dioxide, be understood.

Thermochemical Properties

The heat of formation of carbon dioxide from the elements in their standard states has been determined very accurately by the National Bureau of Standards to be $-94.051 \pm .00108$ Kcal/mole (15). The strength of carbon oxygen bond in carbon dioxide may be derived from the heats of formation of carbon dioxide, carbon monoxide, and oxygen atoms to be 127 Kcal/mole (16). The controversy over the value of the latent heat of vaporization of graphite is not involved in the CO-O bond strength calculation, as is seen below.

$CO_2(g)$	$\rightarrow C(graphite) + O_2(g)$	+94.05 kcal/mole (15)
$C(graphite) + 1/2\ O_2(g)$	$\rightarrow CO(g)$	-26.42 kcal/mole (17)
$1/2\ O_2$	$\rightarrow O(^3P)$	+58.99 kcal/mole (18)
$CO_2(g)$	$\rightarrow O(^3P) + CO(g)$	+126.5 kcal/mole

The ΔH_f^o of carbon monoxide was determined experimentally by combustion. The ΔH_f^o of oxygen atoms was determined spectroscopically.

Spectroscopic Properties

The spectroscopic states and properties of carbon dioxide are summarized in Table II.

TABLE II

SPECTROSCOPIC PROPERTIES OF CARBON DIOXIDE (19)

State	Configuration	Notation	Energy above Ground	Shape
Ground	$\pi^4 g$	$^1\Sigma_g^+$ ($^1A_1$)	0.0 ev	Linear
First observed excited	$\pi^3 g \pi u$	$^1\Delta_u$ ($^1B_2$)	9.5 ev	Bent
First theoretical excited	$\pi^3 g \pi u$	$^3\Sigma_u^+$ ($^3B_2$)	7.6 ev	Bent
First ionization potential			13.769 ev	

Carbon dioxide is very transparent at 1849A at concentrations of one atmosphere and of several decimeters optical path (20). The fundamental frequencies for symmetrical stretching, bending, and asymmetrical stretching vibrations are, respectively, 1388.17, 667.40 and 2349 cm^{-1} (21).

Dissociation

Carbon dioxide dissociates from its (singlet) ground state yielding (singlet) carbon monoxide and (triplet) oxygen by performing a predissociation (22). The vibrationally excited singlet undergoes intersystem crossing to the triplet state, whose activation energy of decomposition is less than that of the singlets, and consequently dissociates. The bond dissociation energy is defined as the difference in enthalpy between the products (CO + O) in their normal vibrational, electronic, and rotational states at 25°C, and the molecule (CO_2) under the same conditions. Carbon dioxide undergoes two major processes of interest upon electron bombardment. Formation of the cation (23), $CO_2 + e^-$ (13.769 ev) $\rightarrow CO_2^+ + 2e^-$, and formation of an anion (24),

$$CO_2 + e^- \text{ (6.7 ev)} \rightarrow CO\ (^1\Sigma_g g) + O^-(^2P_o).$$

Carbon dioxide is very reluctant to form an anion of itself, $CO_2 + e^- \not\rightarrow CO_2^-$, as it has been reported once in minute proportions in mass spectrometry (25), and has been reported to result from the gamma irradiation of formates and, interestingly, of oxalates (26). The CO_2^-

ion has been treated theoretically via MO theory and has thereby been estimated to be non-linear, of the form $C\overset{O}{\underset{O^-}{<}}$. (27)

As mentioned previously carbon dioxide has been shown to be decomposed by ground state sodium and potassium atoms, at elevated temperatures (400°C), to form the respective oxalates. The process has been attributed to displacement of the oxygen by the metal (12). Such a behavior certainly throws suspicion on a charge transfer mechanism as being the cause of the displacement. Of course, carbon dioxide, as described above, is reluctant to form the CO_2^- ion, and the electron affinity of CO_2 for this process has never been measured; however, Mulliken (28) has hypothesized that there need be no requirement of the Lewis acid (CO_2) in charge transfer complexing to exhibit anion formation in order to qualify it as an acceptor.

II.

THE ISOLATION OF MERCURY $6\,{}^1P_1$ ATOMS

THE ISOLATION OF MERCURY 6 $^1P_1$ ATOMS

Synopsis

It is evident from the previous section that in order for photosensitization reactions with mercury 6 $^1P_1$ atoms to be conducted unambiguously, there must be no Hg 6 $^3P_1$ atoms present. Hypothetically, there should be no other extraneous radiation present either (e.g., 1942A, 3130A); however, the absense of Hg6 $^3P_1$ atoms alone will be a significant improvement in the reaction conditions. In order to achieve this goal the ratio of the intensity of 1849A radiation to that of 2537A radiation must be at the very least in the order of ten to one, and preferably one hundred or one thousand to one. To evade these requirements, the mercury vapor pressure could be lowered, since the extinction coefficient of mercury vapor for Hg6 $^3P_1$ resonance radiation is much lower than that for Hg6 $^1P_1$ resonance radiation. However, such a requirement would eliminate one very useful reaction parameter, that of mercury vapor concentration. Therefore, in order to enhance the ratio of Hg6 $^1P_1$ atoms to Hg6 $^3P_1$ atoms in a reactor, the exciting radiation must be appropriately filtered. A knowledge of the relative intensities of 1849A and 2537A radiation of the mercury arcs used in these photosensitization reactions is first necessary so that the requirements of a suitable optical filter may be ascertained. Two types of low pressure mercury arcs were employed. One was a spiral lamp made of suprasil fused quartz with water cooled

•

electrodes and filled with neon (5-10 torr) and mercury droplets. The other lamp was an electrodeless arc made of suprasil fused quartz and filled with a few torr each of neon and argon and mercury droplets. (This lamp was made by W. S. Gleason, formerly of this laboratory). This lamp was sustained by the microwave field of a diathermy apparatus.

The ratio of intensities of 1849A to 2537A radiation for both arcs were found to be approximately one to ten. Thus, for an optical filter to provide the minimum requirements for Hg6 $^1P_1$ photosensitization (ten Hg6 $^1P_1$ atoms to one Hg6 $^3P_1$ atom), its transmission at 1849A must be at least 100 times that at 2537A. One filter was available at the time these experiments were performed, a lithium floride crystal, gamma irradiated by cobalt 60 (31). This filter transmitted with lithium fluoride's usual clarity at 1849A but had an absorption maximum near 2537A caused by "F" centers created by the gamma rays. This filter would have been sufficient for the requirements of these studies except the filter "bleached" with use, that is, the transmission at 2537A increased with exposure to 2537A radiation. The rate of bleaching was found to be too great for practical use in these studies.

An interference filter was reported in 1966 to have been fabricated which may have photochemical resistance and provide good filtration (32). However, it was not available at the time these studies were executed.

The requirements of these studies necessitate a fluid filter, e.g., a solution, since the 1849A intensities are so low that collimating

optical trains, which can accept planar filters (such as LiF or interference type), cannot be used. This is because of the low light collection efficiency of collimating trains using low pressure mercury arcs. Low pressure mercury arcs are not point sources. Annular systems must be employed which collect nearly all of the radiation of an electrodeless lamp or nearly half that of a coiled lamp. Since crystalline LiF and especially interference filters are virtually impossible to manufacture in this form, only a fluid filter can be used. The selection of filter solution media is not difficult. Any of the lower saturated hydrocarbons will suffice (31). The one selected was cyclohexane, mainly because of its anticipated higher solubility for anthracenes, which are to be tried as filters and which are also cyclic. Cyclohexane can be purified by silica gel to yield high transmittance at 1849A.

The selection of a filter solute was readily directed to the anthracenes because of their extremely high $\pi \rightarrow \pi^*$ absorption at 2537A (extinction coefficient of 80,000 to 200,000 liters $mole^{-1}cm^{-1}$)(32), and relatively normal absorption at 1849A (extinction coefficient of 20,000 to 30,000 liters $mole^{-1}cm^{-1}$ (31). However, anthracenes are known to photodimerize and to photooxidize (33). There is also no report of the photochemical stability of the rings of anthracene towards 1849A. Thus, for an anthracene to be employed as a filter, it must be used in a deoxygenated medium, must not dimerize, and must not decompose with near vacuum ultraviolet radiation. The compound finally selected was 9,10 dimethyl anthracene (DMA). Since dimerization of

anthracenes occurred at the 9 and 10 positions, (33)

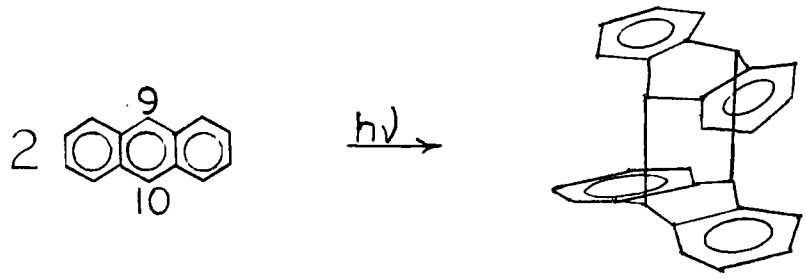

the presence of a substituent at these positions was anticipated to block photodimerization, which the literature and this work verified (34). However, photooxidation of DMA was still evident.

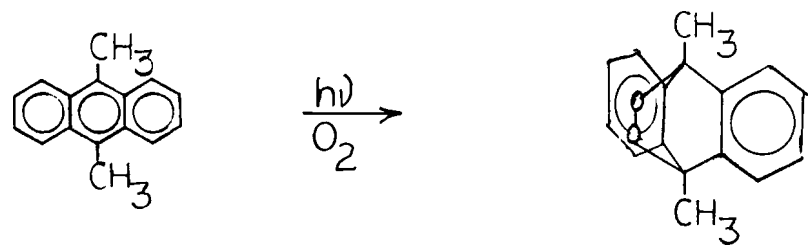

The compound DMA was found to be photochemically stable under 1849A radiation since it maintained its absorbance spectrum quite well when exposed to low pressur e mercury arc radiation (37).

The relationship between transmittance, length, and concentration of 9,10 dimethyl anthracene in cyclohexane solution was found to be as follows:

$$2537A: \quad -\log_{10} T = 0.130 + 8.08 \times 10^{4} \times lc$$

$$1849A: \quad -\log_{10} T = 0.0214 + 1.92 \times 10^{4} \times lc$$

where l = optical path, centimeters

c = concentration, moles liter

and $1.17 \times 10^{-5} < lc < 3.82 \times 10^{4}$.

The above was determined by a least squares treatment of the transmission data.

This filter, 9,10 dimethyl anthracene or "DMA", along with the solvent, water and quartz envelopes present in the optical path between lamp and reactants, can readily achieve a ratio of Hg6 $^1P_1$ atoms to Hg6 $^3P_1$ atoms in the photosensitization reactor that is greater than ten to one, with the overall transmittance of 1849A radiation being from five to ten percent.

Experimental and Results

Performance of Low Pressure Mercury Arcs

The spectra of the arcs were examined on a Seya-Namioka type 0.5 meter vacuum grating spectrograph built by the Jarrell-Ash Co. The use of the instrument was furnished by the NASA Manned Spacecraft Center via the courtesy of R. R. Bilderback, IESD. A lithium fluoride lens was employed at the entrance slit which also served as a vacuum seal. The instrument was operated at around 10^{-3} torr. The optical path from the lamp to the entrance slit consisted of a nitrogen purged lamp enclosure box , approximately 12" cube. A one centimeter cell containing mercury droplets under vacuum was placed between the lamp and the exit of the box, at which a suprasil collimating lens was mounted. The absorption cell could be moved in and out of the beam without considerable admission of air. The cell served to absorb

reversible resonance radiation emanating from the lamp. This permitted measurement of the ratio of reversible to irreversible radiation of both the 2537A line and the 1849A line by difference. Also, the ratio of the reversible radiation of the 1849A line to that of the 2537A line may be thereby determined.

A 12" nitrogen purged cardboard cylinder (empty oatmeal box) was inserted between the lamp's box and the entrance slit to allow sufficient attenuation of the re-irradiated but not transmitted resonance radiation from the mercury cell. This re-irradiated resonance radiation is, of course, undesirable in these measurements. The detector was an end-on photomultiplier. In front of the detector was a plexiglas plate with an opaque layer of sodium salycilate. The coated side of the plate faced the exit slit and the plate itself served as the vacuum seal for the exit slit. This coating has been shown to fluoresce with uniform efficiency for exiting radiation in the range 500A to 3000A (36). The read-out system was assembled by the Jarrell-Ash Company for use with their instrument. It consisted of a power supply, picoampere amplifier, and recorder. The optical layout is depicted in Figure 2.

The electroded spiral arc is depicted in Figure 3. The coil is for ballast and the capacitor for recuperation of power factor. The relative intensity was measured as a function of lamp current. It can be seen that the intensity of the 1849A line increased relative to that of the 2537A line with increasing lamp current.

The electrodeless arc is depicted in Figure 4. The transmission of 1 millimeter of suprasil fused quartz and of 1 millimeter of

FIGURE 2

OPTICAL LAYOUT OF VACUUM SPECTROMETER

Legend:

A Light source under test

B Air tight box, N_2 purged

C Collimating lens (suprasil)

D Absorption cell containing mercury under vacuum (suprasil)

E Light beam

F Spacer, N_2 purged

G Entrance slit

H Vacuum spectrometer

I Grating

J Exit slit

K Plate with phosphor

L Photomultiplier tube

M Power supply, 1500V DC Max

N Picoammeter

O Strip chart recorder

OPTICAL LAYOUT OF VACUUM SPECTROMETER

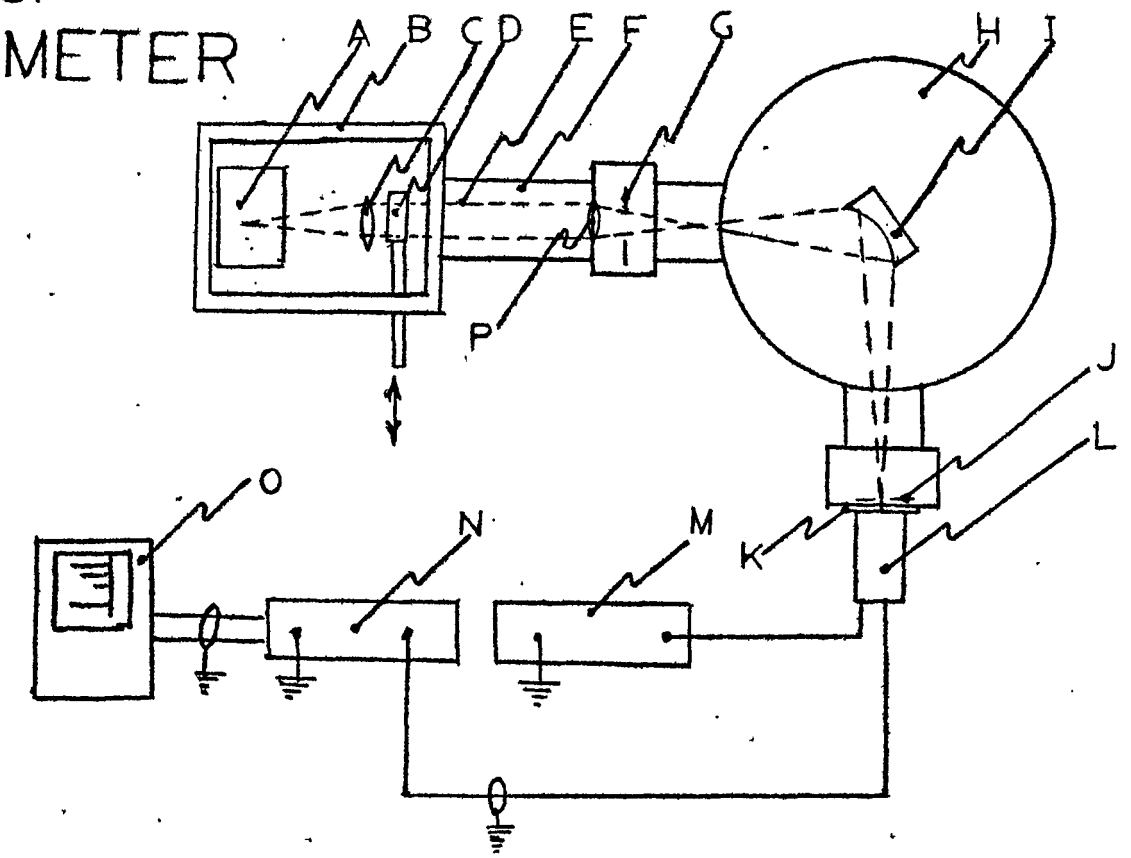

FIGURE 3

SPIRAL ARC

Legend:

A 117 volt AC

B Variable voltage transformer, 1500V AC Max. output

C 1 microfarad capacitor

D 8 henry coil

E Arc

F 0-1000 ma ammeter

G Water cooling jacket (quartz)

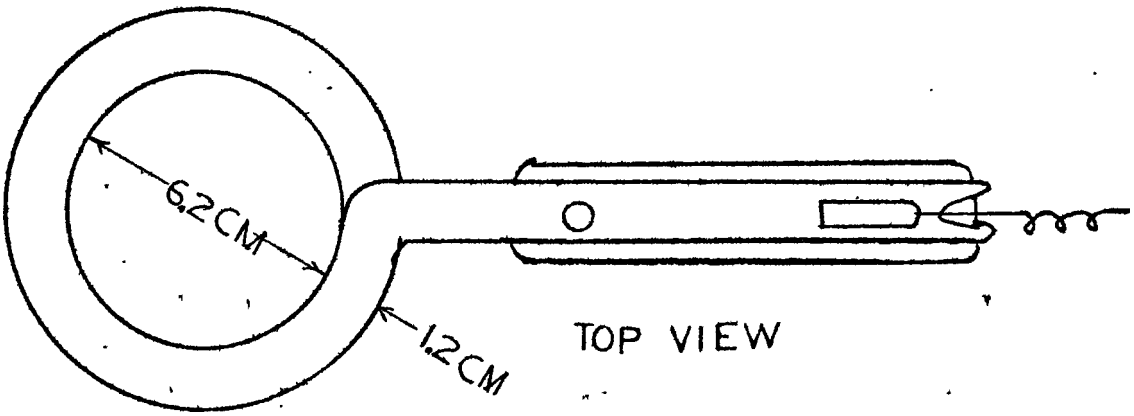

TOP VIEW

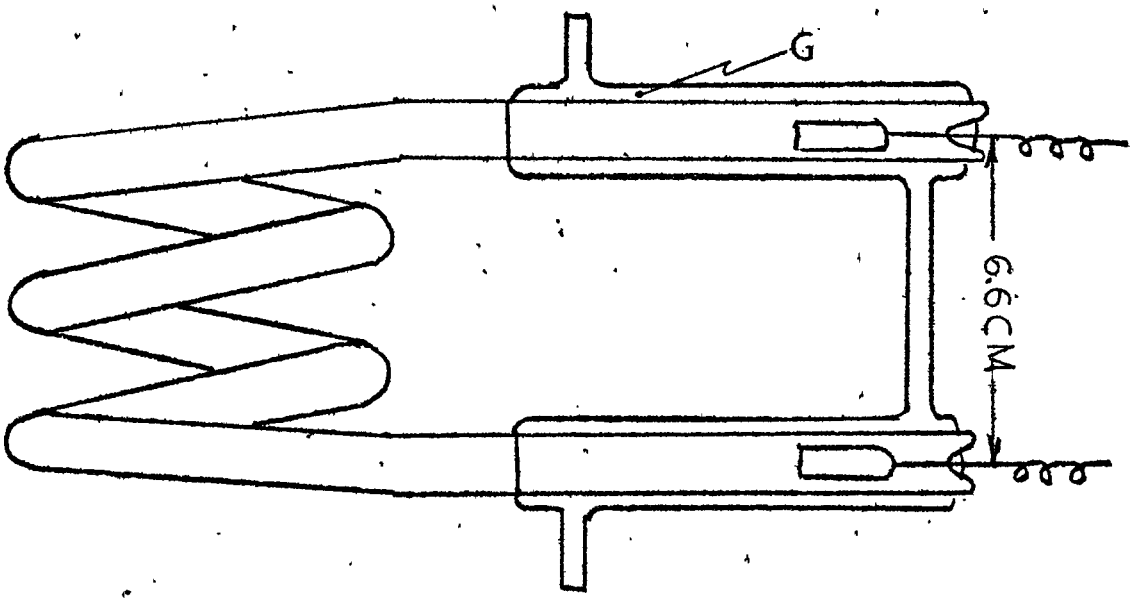

SIDE VIEW

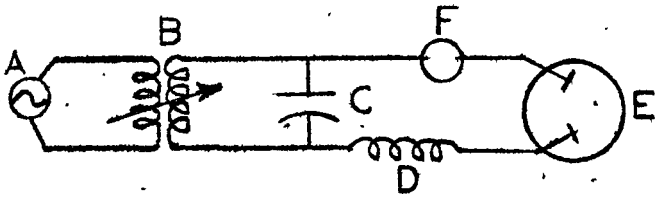

ELECTRICAL SCHEMATIC

FIGURE 3

SPIRAL ARC

FIGURE 4

ELECTRODELESS ARC

Legend:

A Dipole

B Waveguide

C Coaxial cable, to 2450 MHz oscillator

D Electrodeless arc, 8 mm OD x 18 cm

E Cooling water film

F Nylaflow tubing conduit

G Pyrex funnel

H To water drain

I Plexiglas plate

J Aluminum reflector, 1/2 λ radius

K Nitrogen purge port

L Cooling water inlet

ELECTRODELESS ARC

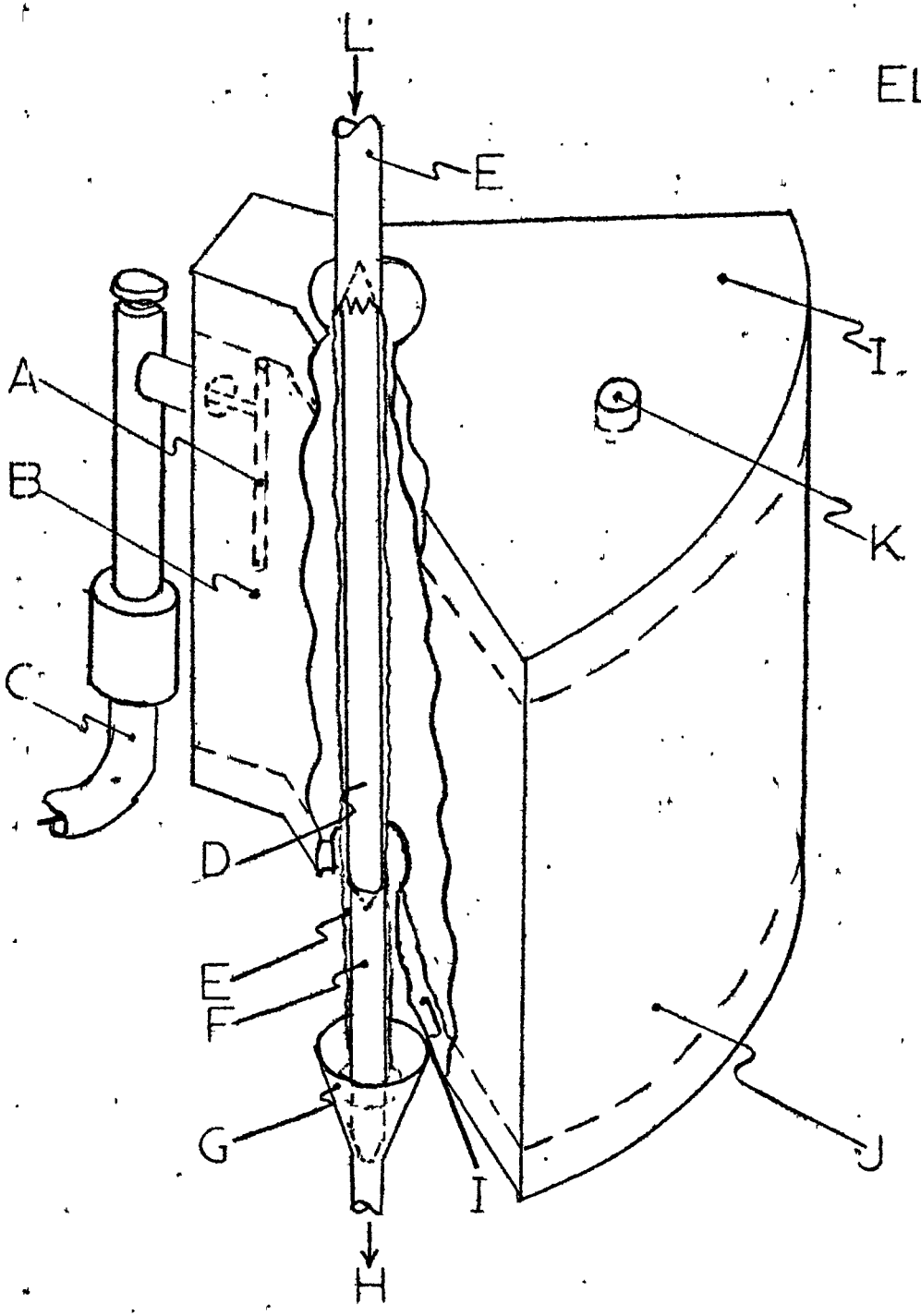

distilled water at 1849A is quite good, as measured by spectrophotometry. The contoured reflector greatly enhanced the brightness of the lamp. The radius of the reflector is half the wavelength of the microwave exciting radiation, forming a resonant cavity. The relative intensities were studied at various water flow rates and, as can be seen in the range of flow rates employed, they had little effect. The water temperature also had little effect in the range 26°C to 30°C.

Three spectral lines were studied in this experiment, those at 1849A, 1942A and 2537A. The line at 1942A was of concern as it was the strongest of the non-resonant lines in the range 1800 to 3000A, and might cause some ambiguities in the reaction. Fortunately, it was at most one-third the intensity of the 1849A line, and the DMA filter absorbs at 1942A with approximately the same magnitude as it does at 1849A. The characteristics of the electroded and electrodeless arcs are described in Tables III and IV, respectively. The intensity ratios are expressed with respect to quanta rather than energy, as the quantum output ratio determines the Hg6 $^1P_1$ to Hg6 $^3P_1$ atom ratio in the reactor. The transmission of the mercury cell was determined on a Cary 15 spectrophotometer and the data were adjusted to nullify its effect.

TABLE III

PERFORMANCE OF THE ELECTRODED (SPIRAL) MERCURY ARC

Current, Milliamps AC	Percent reversible radiation at 1849A	Ratio (of quanta)* 1849A to 2537A	Ratio (of quanta)* 1849A to 1942A
239	97.5	0.095	3.78
322	97.8	0.1145	4.26
323	97.2	0.1035	7.23

*These ratios are those of reversible quanta of the resonance lines.

TABLE IV

PERFORMANCE OF THE ELECTRODELESS MERCURY ARC

Cooling Water, Temperature, °C	Flowrate, Milliliters/sec	Percent Reversible Radiation at 1849A	Ratio (of Quanta)* 1849A to 2537A	Ratio (of Quanta)* 1849A to 1942A
29.95 ± 0.05	0.757		0.0978	4.64
29.95 ± 0.05	8.33		0.1063	3.88
29.95 ± 0.05	11.9		0.1085	3.88
29.9 ± 0.1	0.941	96.9	0.0909	2.79
29.9 ± 0.1	0.212	89.3	0.0410	1.92
29.9 ± 0.1	1.15	96.9	0.0909	3.40
26.12 ± 0.07	1.23	98.0	0.0953	2.98
26.12 ± 0.07	0.682	97.3	0.0908	2.98

*These ratios are those of reversible quanta of the resonance lines.

Evaluation of 9,10 Dimethyl anthracene (DMA) as a Filter

Transmittance

Commercial 9,10-dimethyl anthracene was purified by triple sublimation and samples were weighed to one part in 10^5 on a Cahn microbalance with a five microgram sensitivity. The samples were dissolved in purified, deoxygenated cyclohexane in a nitrogen purged glove box. Each sample was brought to 50.0 milliliters of solution. The samples were to be transferred to a 0.105 millimeter of 1.000 millimeter optical path quartz cell, depending on concentration, and were to be sealed with corks. The transmission of the cells containing solvent were first measured on a nitrogen purged Cary 15 spectrophotometer at 1849A. Nitrogen, no cell versus nitrogen, no cell was established as 100% transmittance. The cells were drained and dried of solvent. They were then filled in the dry box with their respective solutions and their transmittances at 1849A were measured on the nitrogen purged Cary 15 spectrophotometer in the same manner as the empty cells were measured. The transmittance of the DMA is the dividend of the (solution + cell transmittance) by the (solvent + cell) transmittance.

The transmittance at 2537A, which was very low, could not be accurately measured with the Cary 15 spectrophotometer. A special system was built to make these measurements (Figure 5). The multirange feature of the picoamplifier permitted a comparison of the filtered and unfiltered Hg arc beam at 2537A with an accuracy of two

FIGURE 5

APPARATUS FOR MEASUREMENT OF TRANSMITTANCE OF DMA AT 2537A

Legend:

A Light housing

B Hanovia S-100 medium pressure Hg arc

C Optical bench

D Quartz absorption cell containing DNA solution

E Entrance slit

F Hilger monochromator

G Quartz prism

H Scanning drum (manual)

I Exit slit

J Photomultiplier tube, IP 28

K Power supply, 1500V DC

L Picoammeter

M Strip chart recorder

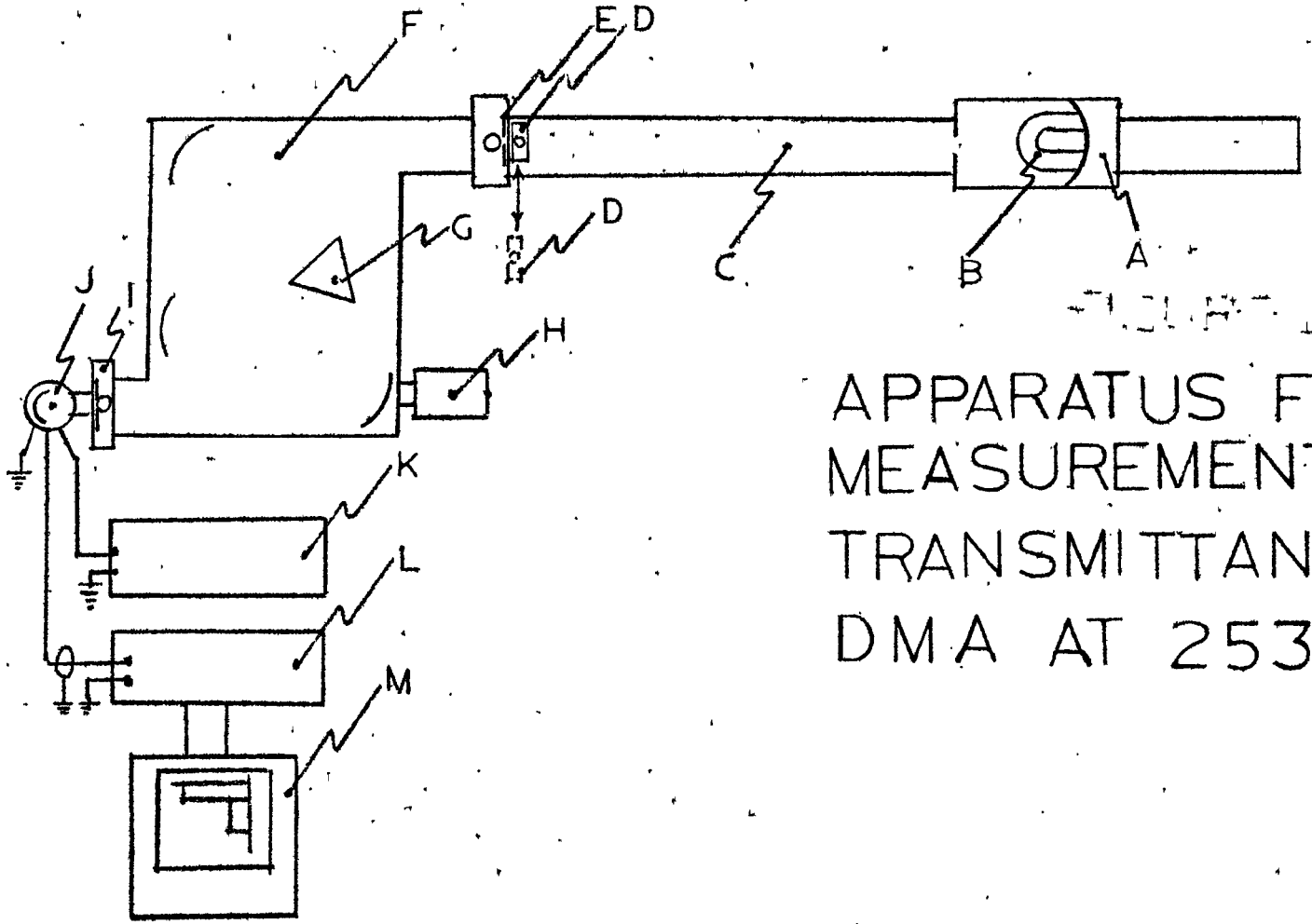

APPARATUS FOR MEASUREMENT OF TRANSMITTANCE OF DMA AT 2537Å

percent; that is, allowed an accuracy of transmittance measurement of two significant figures. The monochromator was simply "peaked" in the vicinity of 2537A on the wavelength drum.

This peak was also the most intense line in the region, although it is reversed. The transmittance was measured in the single beam fashion; the ratio of the photocurrent with the filter in to that of the filter out was the transmittance of the cell and solution. The transmission of the cell and solvent were also measured via this method, and as before, the transmission of the filter was calculated as the ratio of transmittance of cell and solution to that of cell and solvent. The dark current was measured and deducted from the photocurrent in each measurement.

Eight solutions were measured in this manner, four in a 0.105 mm cell and four in a 1.000 mm cell. The transmittances are depicted in Figure 6. The continuous transmittance spectra of DMA of less accurately prepared samples were measured on the Cary 15 spectrophotometer and are depicted in Figure 7.

The relationship between transmittance and the product of concentration and optical path was determined by the least squares method and was found to be as follows:

$$-\log_{10} T1849A = 0.0214 + 1.92 \times 10^{4} \times lc$$

$$-\log_{10} T2537A = 0.130 + 8.08 \times 10^{4} \times lc$$

where T = transmittance

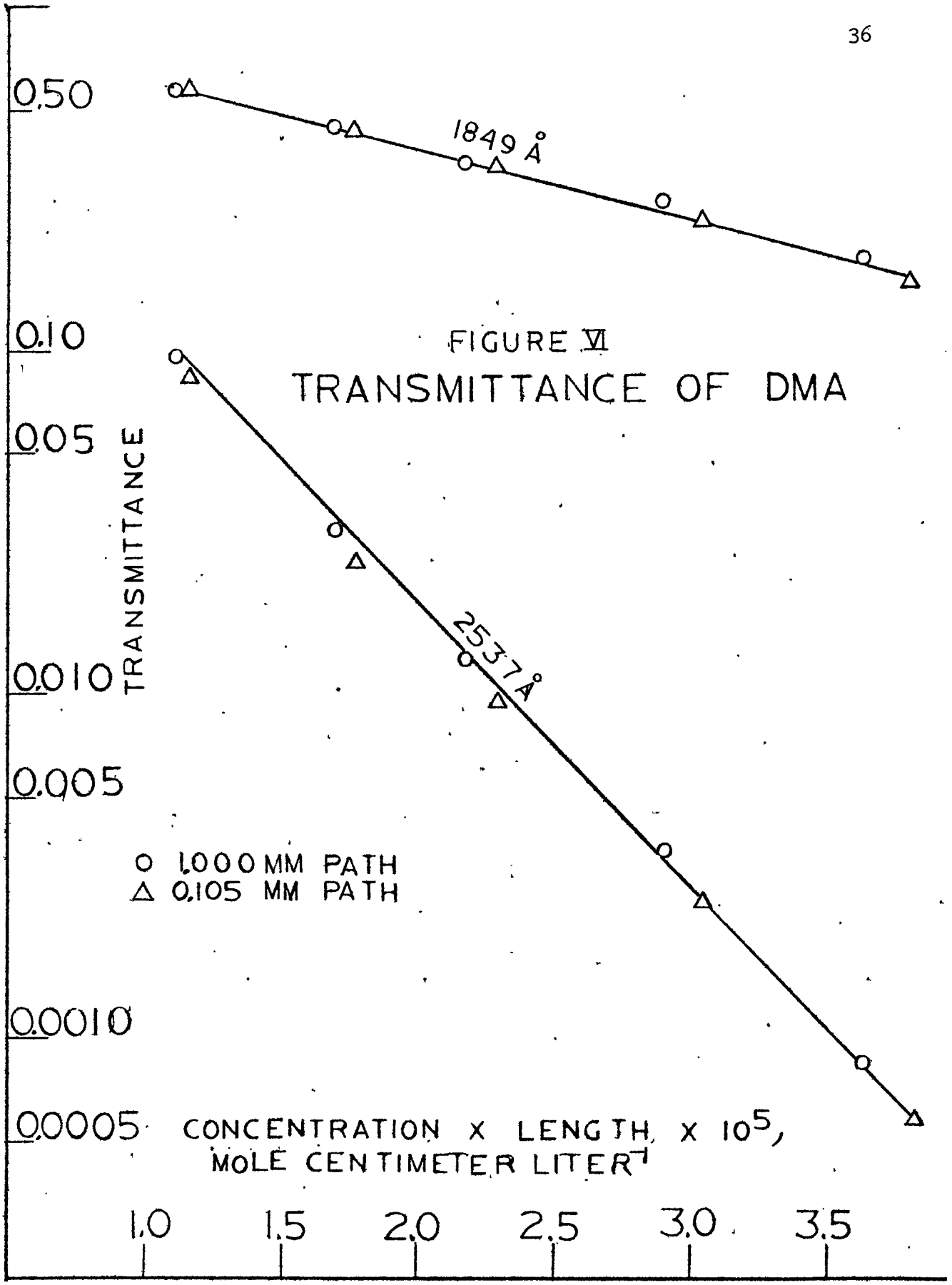

FIGURE VI

TRANSMITTANCE OF DMA

FIGURE 7

TRANSMITTANCE SPECTRA OF 9,10 DIMETHYL ANTHRACENE IN DEOXYGENATED CYCLOHEXANE

Legend:

0.0105 cm Cell with Suprasil Quartz Windows

Concentrations:

A 0.05990 g/liter

B 0.1390 g/liter

C 0.2017 g/liter

Extinction coefficients, liters/mole cm.

$\varepsilon_{2537} = (8.46 \pm 0.13) \times 10^4$

$\varepsilon_{1849} = (1.98 \pm 0.09) \times 10^4$

Cary Model 15 Spectrophotometer

Reference: Nitrogen

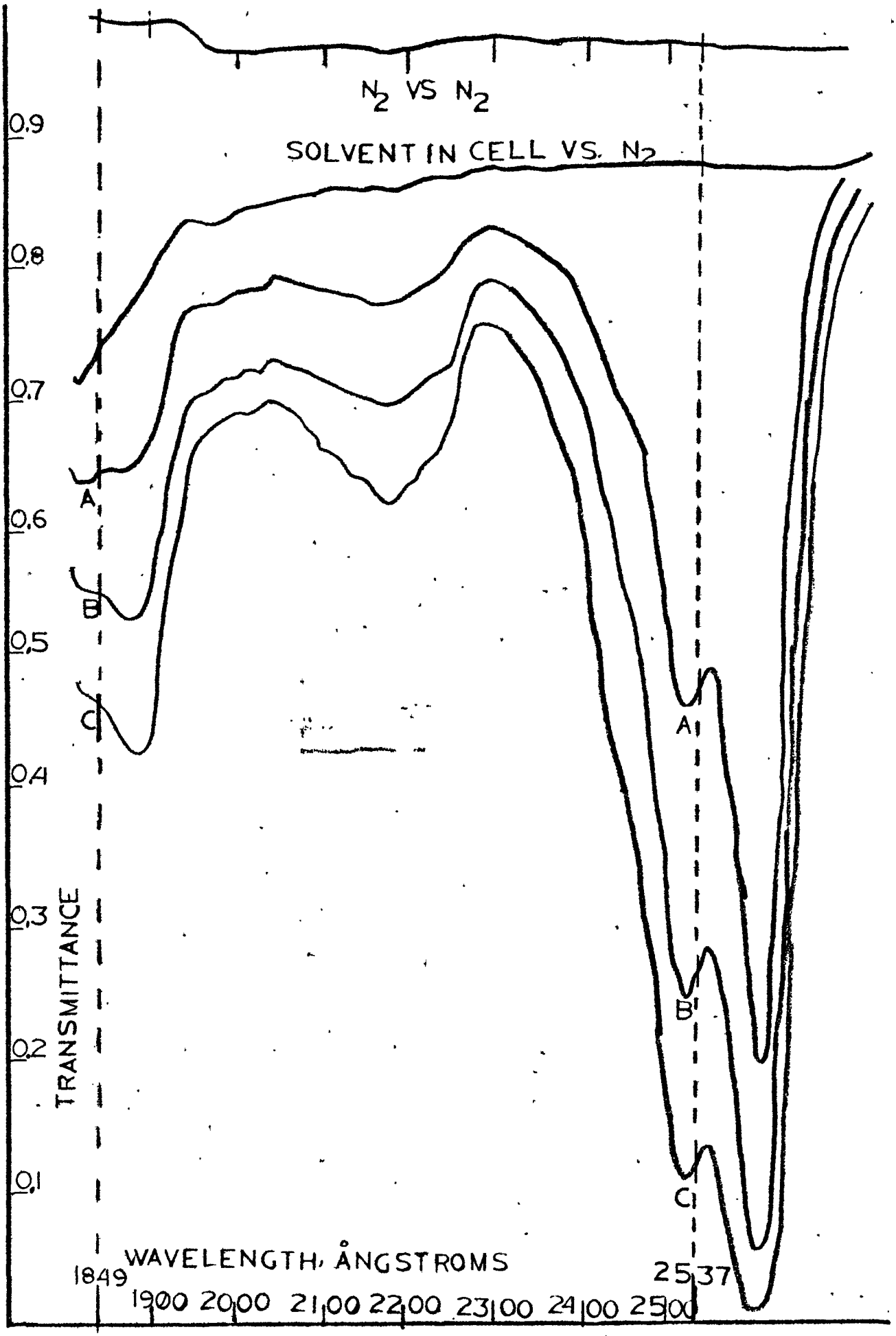
N2 VS N2
SOLVENT IN CELL VS. N2
0.9
0.8
0.7
0.6
0.5
0.4
0.3
0.2
0.1
TRANSMITTANCE
A
B
C
A'
B'
C'
1849
2537
WAVELENGTH, ÅNGSTROMS
1900 2000 2100 2200 2300 2400 2500

l = optical path, centimeters

c = concentration, moles liter

and $1.17 \times 10^{-5} < lc < 3.82 \times 10^{-5}$.

Stability

The stability of a non-deoxygenated cyclohexane solution of DMA under exposure to an electrodeless arc lamp was determined by measuring its transmittance spectrum before and after 90 minutes of exposure. The smooth and dashed lines of Figure 8 depict the transmittance of the filter before and after exposure, respectively. When the solvent was deoxygenated and the cell filled in an oxygen free atmosphere and maintained air tight, the decomposition after nine hours of similar exposure corresponded to a change in 2537A transmittance from 0.0015 to 0.0025 and a change in 1849A transmittance from 0.17 to 0.15, a very slight change for such a long exposure. This change, under conditions identical to that to be employed in the photosensitization reactions, is easily tolerable.

Preparation and Use of the Filter

The technique developed for purification and deoxygenation of the cyclohexane solvent is of such importance that it should be described in detail.

The purification required is the removal of unsaturated impurities which absorb strongly at 1849A. These are probably mostly cyclohexene and some benzene. The impurity removal is performed by passing

FIGURE VIII

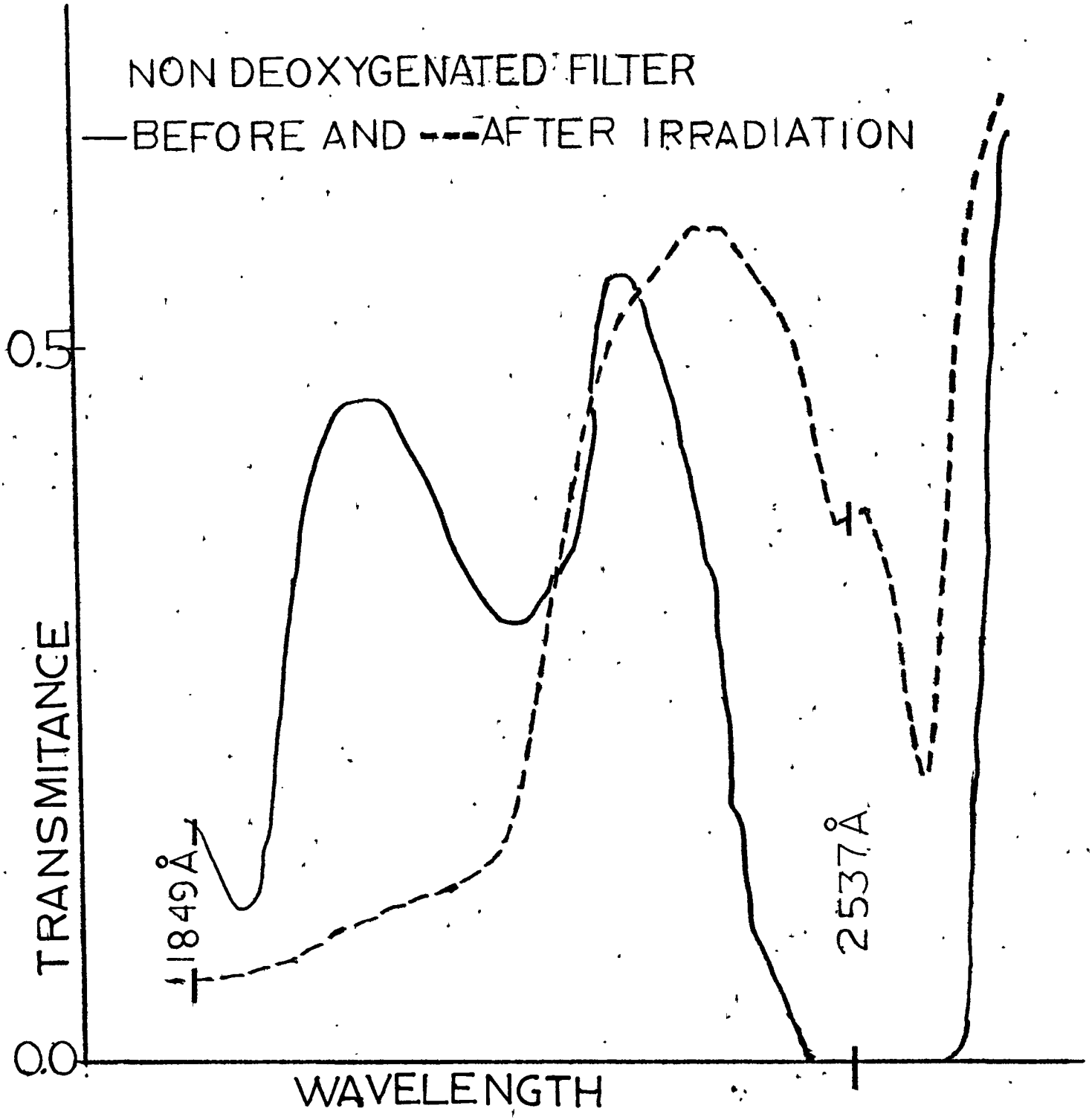
NON DEOXYGENATED FILTER
—BEFORE AND ---AFTER IRRADIATION
0.5
0.0
TRANSMITANCE
1849Å
2537Å
WAVELENGTH

the solvent (spectroquality) several times through a pre-activated column of fine mesh silica. The 1" diameter pyrex column was four feet long with a one liter Florence flash fused to its top as a reservoir. The column is packed with a wad of pyrex wool at the bottom and then filled with about three inches of 5A molecular sieve pellets. The column is wrapped with 1000 watt heating tape and heated while dry nitrogen is purging the column from the bottom. After a half hour of prebaking the column is filled with fine mesh silica gel that has been transferred in pyrex beakers from a muffle furnace, where the beakers and their contents had been baking overnight at 500°C. The column is filled with silica gel while the nitrogen is purging and the column is hot. After the column is filled three inches from the top, the purge is stopped and the rest of the column is filled with more molecular sieve. The column remains heated by the tape for four hours. After cooling, the cyclohexane is transferred from its bottle, which also contains silica gel, into the column. The extreme dryness is necessary because unsaturates are difficult to adsorb, even by silica gel, and, as with any adsorbent, moisture greatly weakens the adsorptive power of the silica gel.

After several cycles through the same column, the now purified cyclohexane is transferred to an "H" tube apparatus for deoxygenation, depicted in Figure 9. The cyclohexane is frozen with liquid nitrogen, the apparatus evacuated, then sealed from the pump. A Dewar flask containing liquid nitrogen is then placed about the empty trap and the cyclohexane in the other trap is driven over by heating the trap with

FIGURE 9

APPARATUS FOR THE DEOXYGENATION OF SOLVENT

Legend:

A Vacuum line

B Greaseless stopcock

C Distillation trap, fixed

D Greaseless "O" ring sealed joint

E Clamp

F Distillation trap, removable

G Dewar flask

APPARATUS FOR THE DEOXYGENATION OF SOLVENT

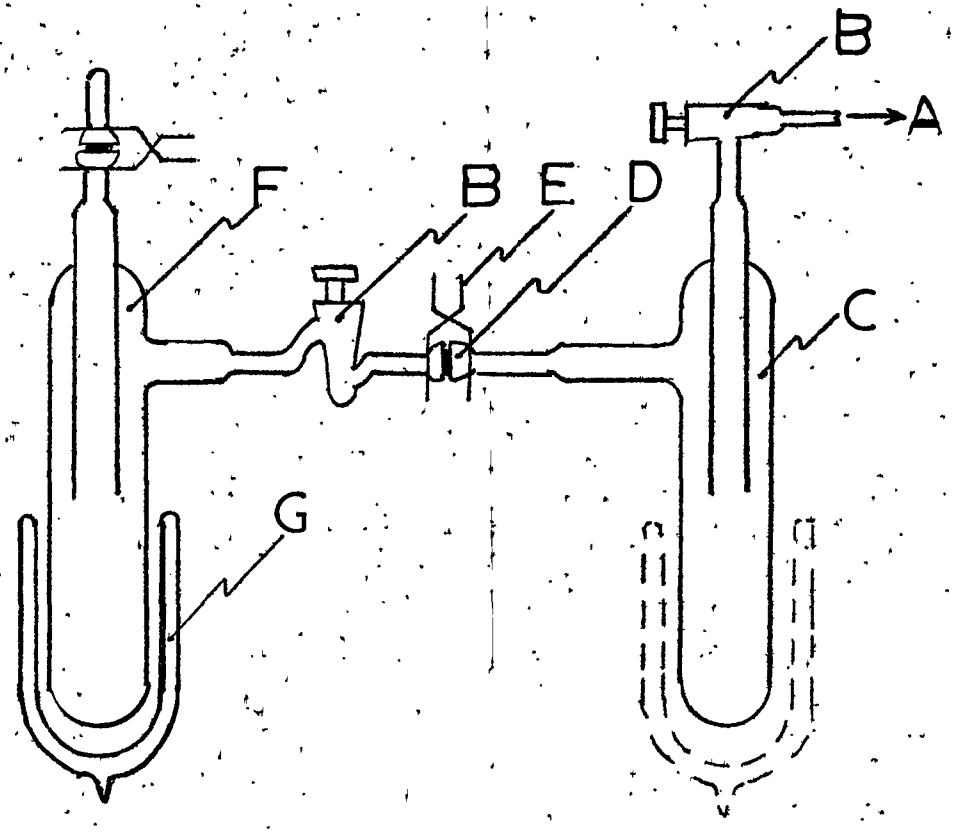

a "heat gun." After transferral, the system is again evacuated, sealed again, and the cyclohexane is transferred back to its original trap by the same distillation process.

The system is then again evacuated with the cyclohexane still solid, the trap containing the cyclohexane is sealed off from the rest of the system, then detached from the system, and transferred to a glove box. The 9,10 dimethylanthracene (DMA) to be dissolved in this cyclohexane is weighed (usually 0.0092 grams) in a 50 milliliter beaker. The beaker and its contents are also transferred to the glove box along with a stainless steel spatula (for assistance in dissolving the DMA), a 50 milliliter volumetric flask, and a pyrex funnel (for transferring the solution into the flask). Also included in the dry box assortment is a specially made filter transfer flask, whose purpose is to transfer the filter out of the nitrogen filled glove box over to the reaction system and into the filter cell. The glove box is then sealed, purged with nitrogen and the trap containing the (melted) cyclohexane is opened. The DMA is dissolved in the 50 milliliter beaker and transferred by washings to the volumetric flask until a solution volume of 50 milliliters is attained. The solution is now ready for delivery to the transfer flask.

The transfer flask is of great practical value in use of the DMA filter, as well as the filter cell system, and both merit a detailed description. It is advantageous to employ a large volume of filter solution in the conduct of the photosensitization reactions since the excessive heat adsorbed by the filter may be dissipated and the effect

of the losses from degradation of the DMA and evaporation of the solvent may be minimized. It is also advantageous to circulate the filter in order to maintain a consistent concentration of DMA in the filter cell and to keep the filter in a nitrogen (inert) atmosphere. A circulation system was designed to provide these features and is depicted in Figure 10. The filter is delivered via funnel from the volumetric flask to the transfer flask in the purged glove box. The transfer flask is then sealed, the glove box opened, and the transfer flask installed in the filter system. The system is purged by passing nitrogen into the socket joint arm, down through its three-way stopcock on the arm with the ball joint into the circulating system. The nitrogen circulating purge at the bottom of the system is also turned on. After ten minutes or more of purging, the three-way stopcock on the arm with the ball joint is turned to open the contents of the flask to the circulation system and the nitrogen purge is also diverted into the flask to displace the contents of the flask into the circulating system. The nitrogen entering from the bottom of the system circulates the filter by displacement and the nitrogen entering from the transfer flask maintains the nitrogen purge in the system. Samples of the filter may be drawn from the stopcock at the bottom of the system for the purpose of monitoring the filter transmittance during the reaction via spectrophotometer. It is seen that the filter is never exposed to air from preparation to application.

FIGURE 10

FILTER CELL AND CIRCULATION APPARATUS

Legend:

A N_2 inlet, transfer filter and purge

B Threeway stopcock

C Threeway stopcock

D 12/5 Ball and socket joint

E Filter transfer flask

F Latex tubing

G Reservoir

H N_2 exhaust nozzle

I N_2 inlet, circulate and purge

J Filter sampling tap

K Direction of circulation of filter

L Filter jacket

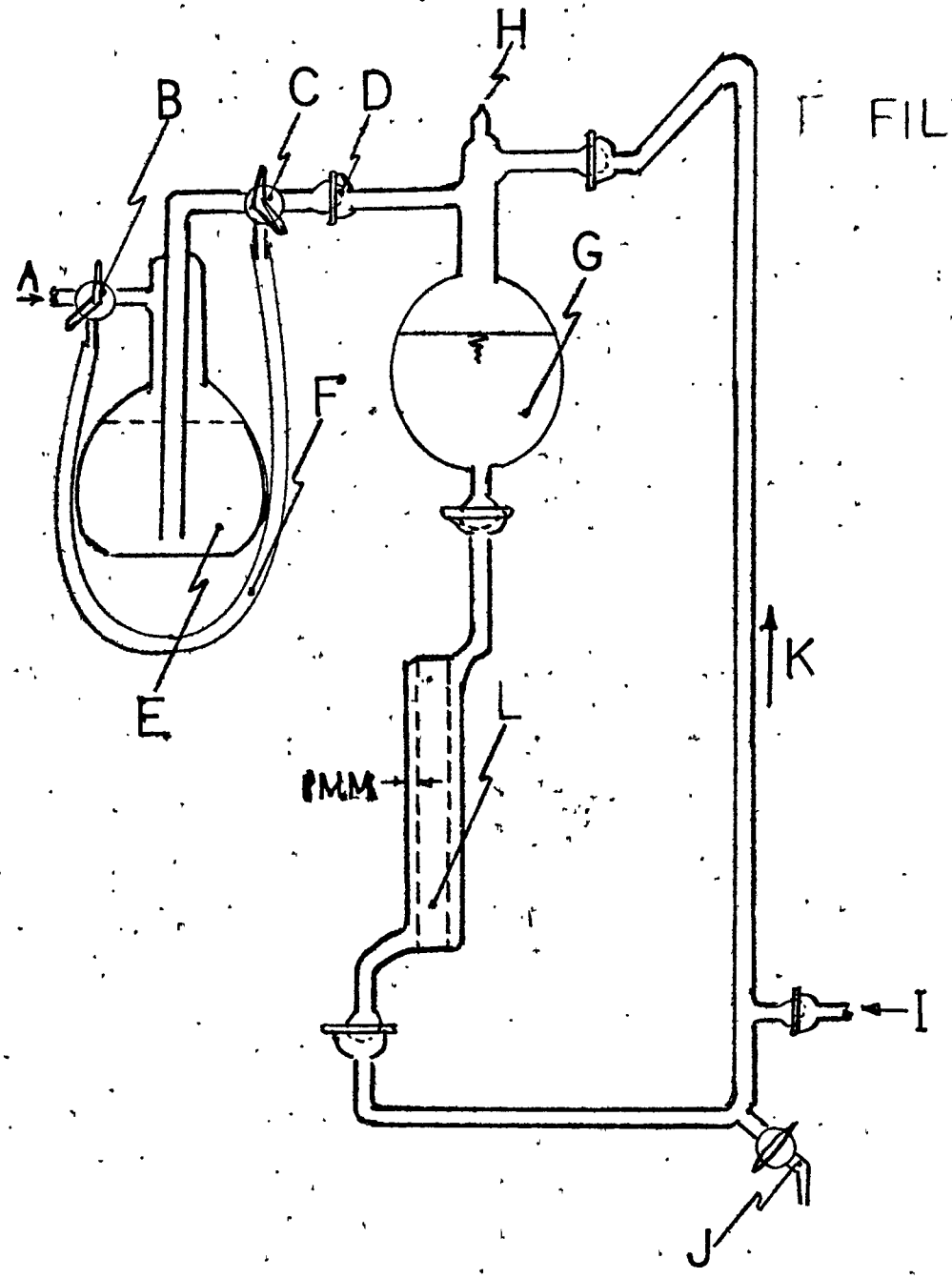

FILTER CELL & CIRCULATION APPARATUS

III.

THE PHOTOSENSITIZED DECOMPOSITION OF CARBON DIOXIDE WITH MERCURY 6 $^1P_1$ ATOMS

THE PHOTOSENSITIZED DECOMPOSITION OF CARBON DIOXIDE WITH MERCURY 6 $^1P_1$ ATOMS

Synopsis

In this research the identity of the products was first established, then the mechanism of their production was investigated. This mechanism was kinetically elucidated by studying the effect of carbon dioxide pressure, mercury pressure, reaction time, and the excitation spectrum on the yield of products. The photochemical behavior of the products was also studied as an aid in understanding the reaction.

Analysis of the Products

The gas phase products of the reaction were analyzed by gas chromatography. They were found to be composed only of carbon monoxide. No oxygen was detected, where the chromatographic columns employed were shown to easily resolve oxygen, nitrogen, and carbon monoxide, and of course, carbon dioxide. A special experiment was performed at low mercury pressure, which would decrease, if not nullify, any scavenging of atomic oxygen by mercury, but the gas phase still remained composed of only carbon monoxide.

The solid phase products were more interesting. Each reaction that yielded extensive carbon monoxide in the gas phase also yielded a brownish yellow to yellow colored film on the reactor. This behavior, along with the formation of only carbon monoxide in the gas

phase, was reported in previous experiments in the mercury 6 $^1P_1$ photosensitization of carbon dioxide. However, when the film was mildly pyrolyzed under vacuum (250°C), the yellow color remained but the pressure in the reactor increased. The contents of the cell were then analyzed by gas chromatography and found to be carbon dioxide. After the cell was re-evacuated, the remaining film was pyrolyzed at high temperatures (600-800°C) and the yellow film disappeared. The pressure in the reactor increased, and its contents were analyzed by gas chromatography to be only oxygen. This left little doubt that the yellow film was mercuric oxide.

The identity of the solid material that yielded carbon dioxide on pyrolysis remained of great interest. Two experiments were run that verified that the carbon dioxide found was actually a reaction product and not simply reagent carbon dioxide that was adsorbed on the reactor wall. In one, a "photosensitization" reaction was performed under the identical conditions of that reaction which yield the product in question, except that no light was used. The reactor was then evacuated and sealed. No significant increase in pressure in the reactor was detected after first mild and then severe pyrolysis. The other experiment was performed to verify that carbon dioxide was not adsorbed on the mercuric oxide film. A gas chromatograph column consisting of three feet of powdered mercuric oxide was prepared. The retention time of carbon dioxide in this column was the same as that for air. Thus, since silica gel columns have considerable retention for

carbon dioxide whereas the silica reactor wall did not, it is safe to conclude that if a mercuric oxide column would not retain carbon dioxide, a mercuric oxide coating on the reactor wall would not either.

The possible compounds containing mercury, carbon, and oxygen, or carbon and oxygen and yielding carbon dioxide on pyrolysis are, fortunately, few in number. They are as follows:

Mercuric carbonate 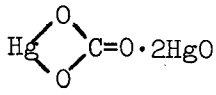

Mercurous carbonate 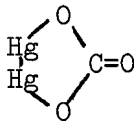

Mercuric oxalate 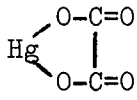

Mercurous oxalate 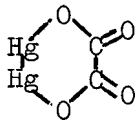

Carbon dioxide O=C=O

The carbonates pyrolyze yielding oxides of mercury and carbon dioxide. The oxalates of mercury were shown by experiment to yield carbon dioxide, and small amounts of carbon monoxide. The quantity of carbon dioxide produced on pyrolysis was so small that an amount of carbon monoxide proportional to that found in oxalate pyrolysis was not detectable. Adsorbed carbon dioxide was ruled out

by the previously described experiment. Thus it became a question of discerning between the carbonates and oxalates of mercury. The diphenylamine blue test can discern oxalates from carbonates (38). The film on the reactor from a photosensitization reaction yielding a significant amount of carbon monoxide was washed from the reactor with dilute HCl, the solution was allowed to evaporate, and the residue when melted with diphenylamine yielded a blue lake, the positive test for oxalate. To verify further the identity of the solid as an oxalate, the product was tested to reduce permanganate. Oxalates will reduce permanganate ion but carbonates will not (39). The mercury of the acid washings of a reactor was first precipitated as sulfide to remove any oxidizable mercurous compounds, if any, and the pre-boiled supernatant, when mixed with an aliquot of very weak permanganate, was found by spectrophotometry, and visibly, to have reduced the permanganate. The type of oxalate, i.e., mercuric or mercurous, could never be determined analytically; however, it was elucidated kinetically as mercuric oxalate, HgC_2O_4. The literature also lends credibility to the formation of an oxalate of mercury by photosensitization of carbon dioxide. As mentioned in the Introduction, Drechsel (11) and Lemarchands and Roman (12) reported the formation of sodium and potassium oxalates when mixtures of sodium vapor or potassium vapor, respectively, and carbon dioxide were passed over powdered silica at 400°C. Since the ionization potentials of these alkalies are quite low, it is apparent that the

valence electron could be easily transferred to the carbon dioxide forming a radical

$$M + O = C = O \rightarrow \overset{\delta+ \quad \delta-}{M - O - C = O}$$

which could combine with another similar radical forming an oxalate

$$\overset{+ \quad -}{2M - O - C - O} \rightarrow \overset{\delta+ \quad \delta-}{\begin{matrix} M - O - C = O \\ M - O - C = O \end{matrix}}$$

Such a reaction would not be feasible with normal mercury atoms, since their ionization potential is too high; however, this reaction is theoretically possible for excited singlet mercury atoms, since their ionization potential is in the range of alkalies.

TABLE V

IONIZATION POTENTIALS OF SOME ATOMS

ATOM	IONIZATION POTENTIAL
Na2 $^2S_{1/2}$	5.14 ev (40)
K3 $^2S_{1/2}$	4.40 ev (40)
Hg6 ^1S_o	10.43 ev (40)
Hg6 $^3P_1$	5.53 ev
Hg6 $^1P_1$	3.72 ev

Still another interesting property of the reactor film is its behavior in photolysis. When a large amount of film was built up in a reactor, the reactor evacuated, and the film photolyzed with the low pressure mercury arc unfiltered, the film yielded carbon dioxide and carbon monoxide in the gas phase. When the experiment was repeated and the film photolysis was conducted for a longer time, the gas phase product was only carbon monoxide. The most likely explanation is that the film initially photolyzes yielding carbon dioxide and mercury, and the carbon dioxide and mercury then undergo the gas phase photosensitization process yielding mercuric oxide and carbon monoxide. To relate this phenomenon to the behavior of oxalates of mercury, mercuric and mercurous oxalates were synthesized and photolyzed by a low pressure mercury arc and a medium pressure mercury arc. For all cases, carbon dioxide was the predominant product. The photolysis with the low pressure arc yielded a considerably higher amount of carbon monoxide relative to carbon dioxide than did photolysis with the medium pressure (reversed) mercury arc. Thus the behavior of the oxalates of mercury agreeswith the behavior of the photosensitization product films.

Effect of the Filter

The discovery of the oxalate in the film leads to the question of whether the film is peculiar to the photosensitization reaction employing a filter or rather the oxalate was just overlooked in the

previous investigations of this reaction which did not use optical filters. To answer this question, several reactions were performed without the use of a filter. In each case, only carbon monoxide was detected in the gas phase, and the yellow film was present but did not yield any carbon dioxide on pyrolysis. A very plausible explanation of this phenomenon is that the 2537A radiation, which is ten times as intense as the 1849A radiation, decomposed the oxalate as soon as it was formed. The filtering removed this component and would subject the film only to the 1849A radiation that created the film and to the 1942A radiation, which is about half the intensity of the 1849A radiation, and the much weaker lines, and therefore allow it to exist.

A reaction was carried out using methanol as a filter. Methanol's shortwave cut off was measured to be between 1900 and 2000A in a one millimeter cell; thus this reaction would indicate the decomposition of carbon dioxide caused by Hg6 $^3P_1$ photosensitization and photolysis from other mercury lines. The results of the reaction showed a fairly heavy yellow film on the portion of the reactor not covered by the filter but exposed to the arc's radiation, whereas that portion of the reactor shielded by the filter had no deposit. It is concluded that carbon dioxide was not significantly decomposed by radiation of wavelengths greater than 1900A. This is also verified by the results of Strausz and Gunning (7) and Cline and Forbes (6).

Kinetics of the Reaction

Preface to the Synopsis of the Kinetics of the Reaction

One general characteristic of nearly all of the quantitative reactions performed is that the yield of carbon monoxide formed relative to the intensity at 1849A gave attractive data; that is, straight lines or smooth curves. The solid phase oxalate, analyzed as CO_2 from pyrolysis of the reactor, gave less attractive results, and the solid phase mercuric oxide yield analyzed as the oxygen from the pyrolysis of the reactor gave quite unattractive quantitative data, as it refused to adhere to any regular pattern. Also, in all cases the mercuric oxide analyzed never equalled its equivalent (one-half) amount of gas phase carbon monoxide. This may be attributed to the fact that some of the oxygen atoms formed from mercuric oxide pyrolysis probably recombined with the mercury left in the reactor, causing a deficient analysis. Mori (8) and Wijnen (9) also reported deficiencies in the oxygen analysis of carbon dioxide photolysis products. They attributed this deficiency to adsorption of oxygen on the reactor walls. The marginal appearance of the oxalate yield data may be related to the behavior of the mercury arc in other portions of the spectrum, particularly the mercury spark lines (including that at 1942A) whose relative intensities are not nearly as reproducible in repeated arc burnings as are those of the arc lines. This was found to be very likely in the "multiple reactor" runs where four

reactors exposed to the same burning of the same lamp gave very coherent data with respect to each other, but on a different run gave mutually coherent data that was not coherent with the mutually coherent data of the previous burning. These spark lines also contribute to the decomposition of the oxalate. Therefore, the conclusions of this research will be derived mainly from the yield of gas phase carbon monoxide products relative to the intensity of 1849A. This quantity is obtained by dividing the pressure of gases non-condensable in a liquid nitrogen cooled trap by the average transmittance of the filter at 1849A during the reaction. This number is usually expressed only in significant figures; that is, the order of magnitude is not expressed. This assumes, of course, that the intensity of the lamp at 1849A is the same for all reactions. It should be pointed out here that such was found not to be the case. The lamp's intensity at 1849A became variable with the use of the lamp, as found by the author and by W. S. Gleason also of this laboratory, who was employing a multitude of these lamps, which he ably manufactured, at the time of this research. It became very apparent, toward the end of this research, that in order to attain reliable quantitative data, several reactors must be exposed to the same lamp at the same time, or in the case of timed runs, during the same ignition. A reaction system was devised that provided this feature from which the data on carbon dioxide pressure dependence and time dependence at mercury vapor pressures corresponding to room temperature liquid were obtained.

The data on mercury vapor pressure dependence, 1849A intensity dependence, and high carbon dioxide pressure dependence and some special experiments were taken by repeated exposures (lamp ignitions) in a single cell, and as the number of exposures increased, the data, although still sufficient for demonstration of the reaction's behavior, became less reproducible. With this preface in mind, the kinetics of the reaction shall be described.

Effect of the Intensity of the 1849A Line

The effect of the intensity of the 1849A line on the yield of products is described in Table VI.

TABLE VI

YIELD OF PRODUCTS AS A FUNCTION OF 1849A INTENSITY

Pressured carbon dioxide - 20 torr. Reaction time - 30 minutes
Mercury temperature = 22°C.

Transmittance of Filtered 1849A	Yield of CO(g)-T* (relative)	Yield of Oxalate(s) ÷ T* (relative)	Yield of Oxalate(s) ÷ T^{2*} (relative)
0.0315	11.00	3.38	1.07
0.0227	11.07	3.22	1.47
0.0286	11.33		
0.0413	11.31		
0.0527	11.07	3.74	0.71

*T = transmittance of filter at 1849A.

Since the yield of carbon monoxide relative to the filter transmittance at 1849A is constant, the yield of gas phase carbon monoxide is directly proportional to the 1849A intensity. The 1849A intensity dependence of the formation of oxalate is not as exact; however, it is reasonably apparent that it is probably linearly related to the 1849A intensity.

If it is postulated that the formation of an excited complex results from collision of a Hg6 $^1P_1$ atom with a carbon dioxide molecule;

$$HgP_1 + CO_2 \rightarrow HgOCO^* \qquad (1)$$

The complex may either decompose forming the carbon monoxide:

$$HgOCO^* \rightarrow HgO + CO\ (g) \qquad (2)$$

or collide with another complex molecule forming oxalate:

$$2\ HgOCO^* \rightarrow Hg_2C_2O_4 \qquad (3)$$

or collide with a carbon dioxide molecule to form oxalate:

$$HgOCO^* + CO_2 \rightarrow HgC_2O_4 \qquad (4)$$

Should any oxalate be formed, it would be decomposed by irradiation at 1849A and by other spectral lines emanating from the lamp through the filter and in the ultraviolet

$$h\nu + Hg_x C_2O_4 \rightarrow Hg + 2CO_2,\ x=1 \text{ or } 2 \qquad (5)$$

Reaction (2) is proportional to T_{1849}

Reaction (3) is proportional to T^2_{1849}.

Reaction (4) is proportional to T_{1849}

Reaction (5) is proportional to T_{1849} and the intensities of the other spectral lines of the arc in the ultraviolet and the corresponding filter transmittances.

The linear relationship of CO formation to T_{1849} indicates reaction (2) is a probable step. Likewise, the linear relationship of oxalate formation indicates that reactions (4) and (5) are probable steps regulating the appearance of oxalate, and thus that oxalate is probably mercuric oxalate.

Effect of Carbon Dioxide Pressure

The effect of the carbon dioxide pressure on the relative quantum yield of product formation; i.e., the yield of product divided by T1849, is described in Table VII and is depicted in Figures 11 through 14.

It is seen that the yield of CO (g), and somewhat less rigidly that of oxalate, reaches a high pressure plateau in all three cases, and that in the first two cases, the plateau begins at about 5 torr CO_2 pressure and that in the third case, that of multiple reactors, the plateau begins at about 1 torr CO_2 pressure. To explain these phenomena, the mechanism postulated in the previous section is recalled for further refinement. Let the radical formation step again be

FIGURE 11

PRODUCT RATES AS A FUNCTION OF

CARBON DIOXIDE PRESSURE

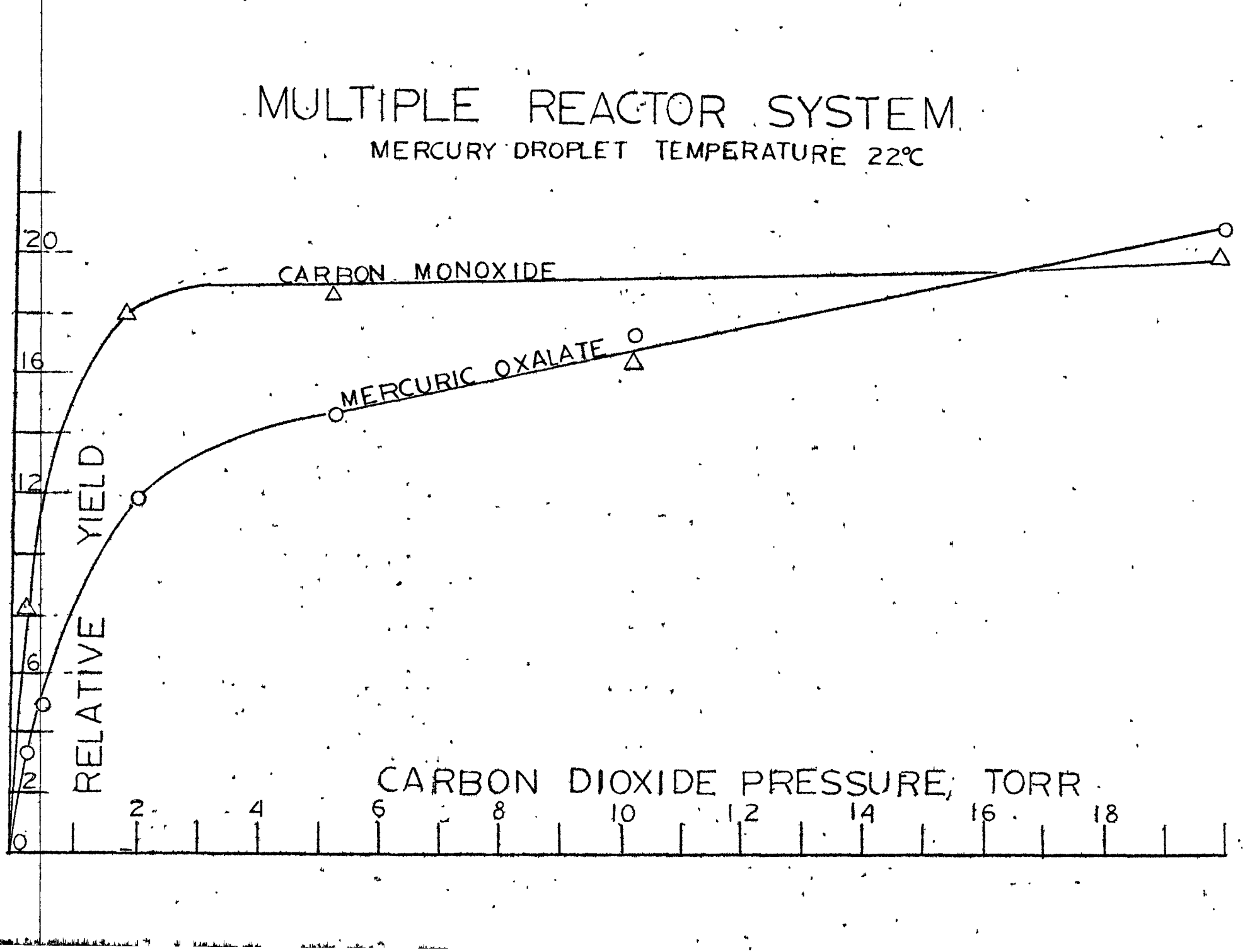
MULTIPLE REACTOR SYSTEM
MERCURY DROPLET TEMPERATURE 22°C
CARBON MONOXIDE
MERCURIC OXALATE
RELATIVE YIELD
CARBON DIOXIDE PRESSURE, TORR
0
2
6
12
16
20
2
4
6
8
10
12
14
16
18

FIGURE 12

PRODUCT RATES AS A FUNCTION OF

CARBON DIOXIDE PRESSURE

MULTIPLE REACTOR SYSTEM

MERCURY DROPLET TEMPERATURE 22°C

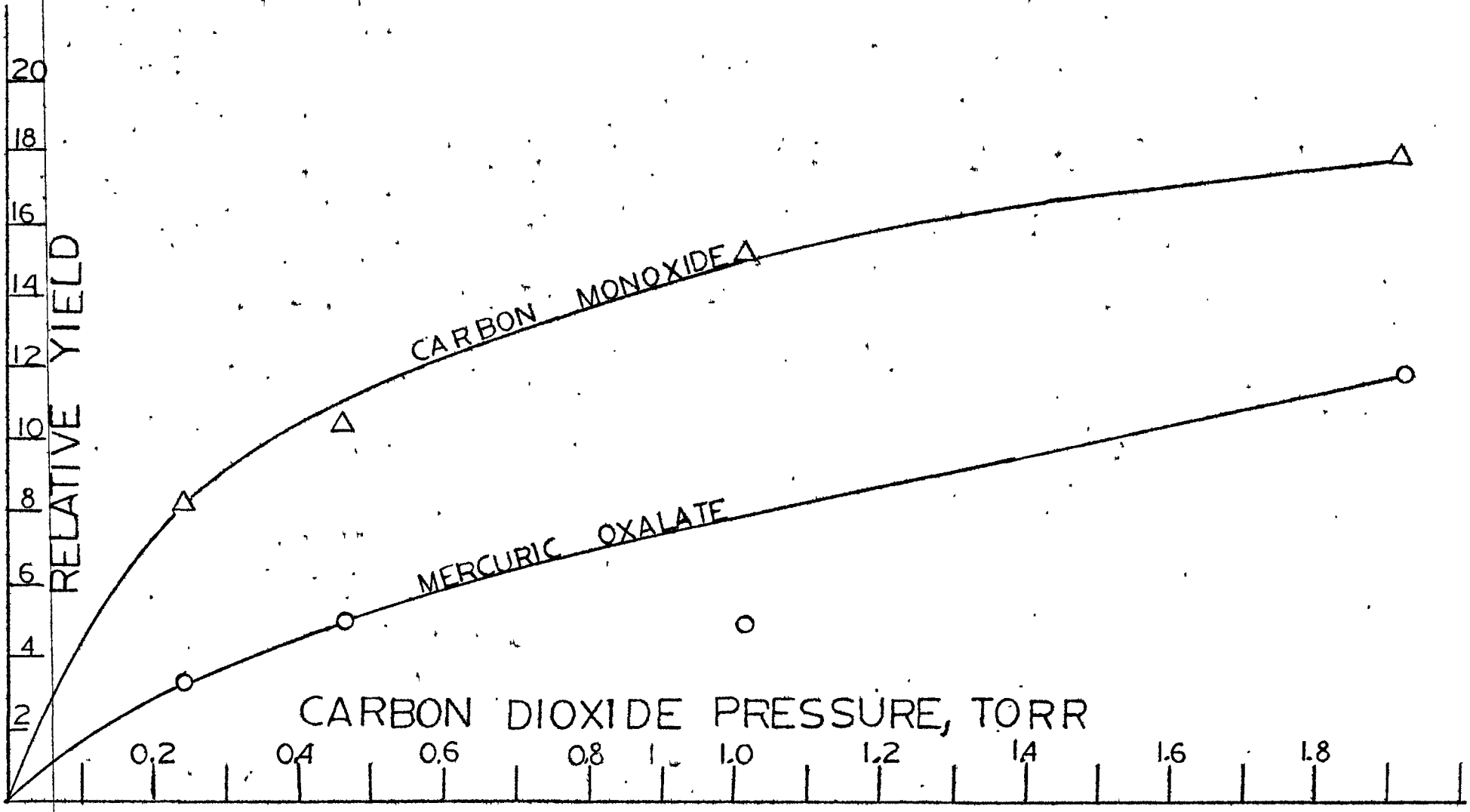

FIGURE 13

PRODUCT RATES AS A FUNCTION OF

CARBON DIOXIDE PRESSURE

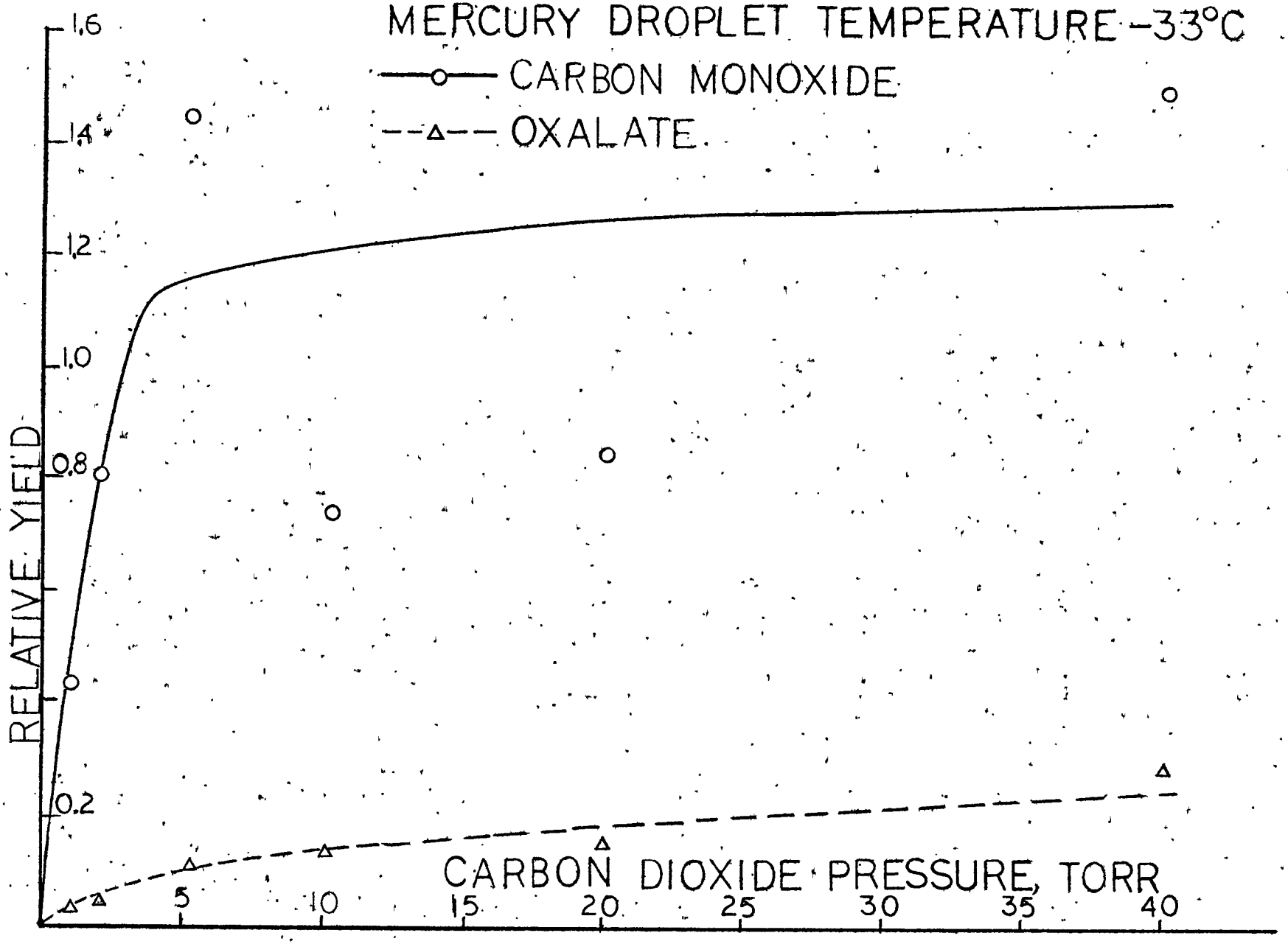
SINGLE REACTOR SYSTEM
MERCURY DROPLET TEMPERATURE -33°C
CARBON MONOXIDE
OXALATE
RELATIVE YIELD
1.6
1.4
1.2
1.0
0.8
0.2
CARBON DIOXIDE PRESSURE, TORR
5
10
15
20
25
30
35
40

FIGURE 14

PRODUCT RATES AS A FUNCTION OF

CARBON DIOXIDE PRESSURE

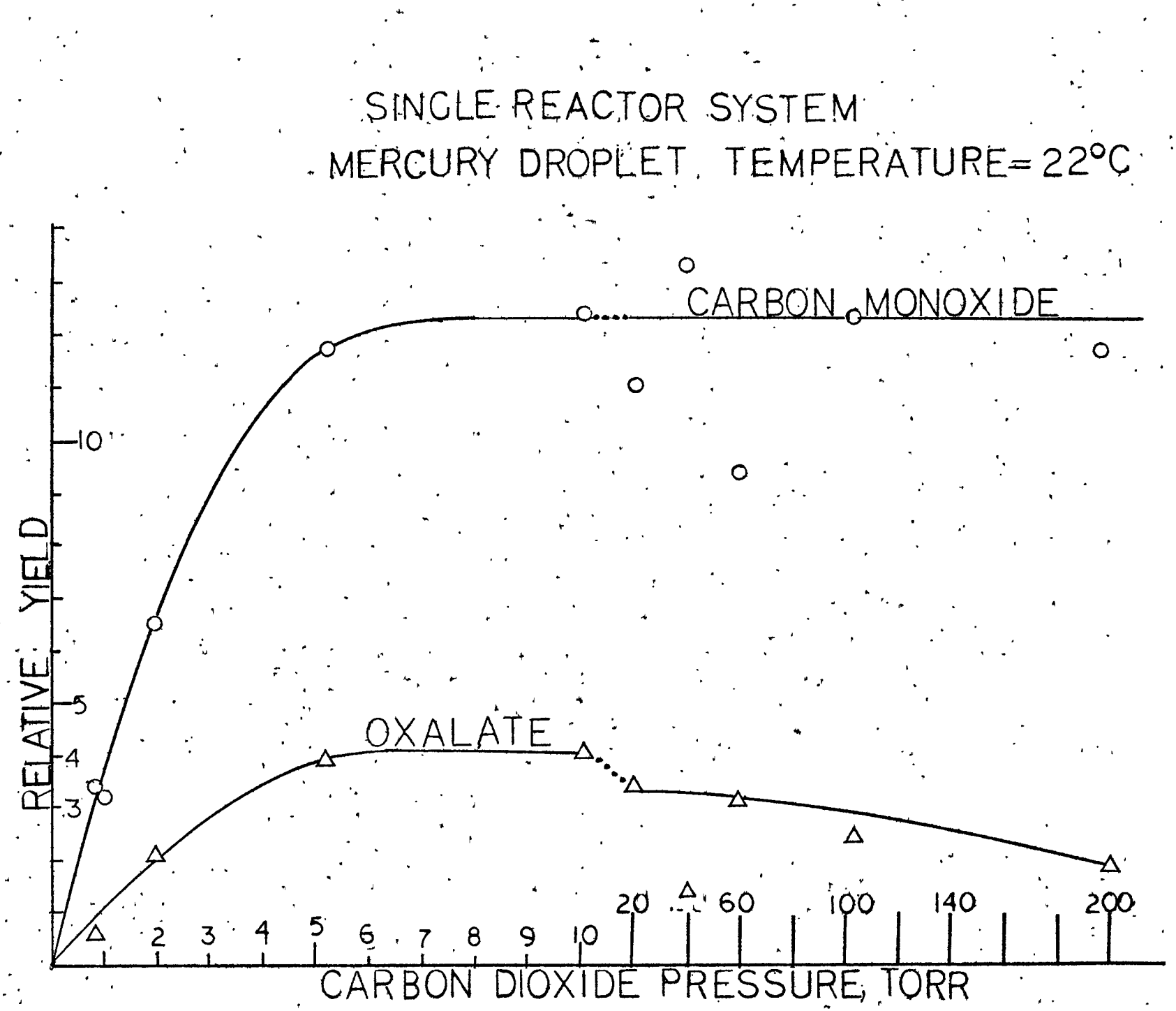
SINGLE REACTOR SYSTEM
MERCURY DROPLET, TEMPERATURE = 22°C
CARBON MONOXIDE
OXALATE
RELATIVE YIELD
10
5
4
3
2
3
4
5
6
7
8
9
10
20
60
100
140
200
CARBON DIOXIDE PRESSURE, TORR

TABLE VII

RELATIVE QUANTUM YIELD OF PRODUCTS AS A FUNCTION OF CARBON DIOXIDE PRESSURE

Carbon Dioxide Pressure, torr	Relative Yield of CO(g)	Relative Yield of Oxalate(s)
Mercury Droplet Temperature = -33°C, single reactor system*		
0.973	0.413	0.0282
1.940	0.806	0.0442
5.1	1.45	0.102
10.1	0.741	0.142
20.1	0.848	0.149
40.7	1.510	0.288
Mercury Droplet Temperature = 22°C, single reactor system*		
0.803	3.36	0.537
0.983	3.17	
1.930	6.45	2.08
5.2	11.67	3.86
10.8	12.33	3.97
20.1	11.00	3.38
39.6	13.3	1.36
61.0	9.32	3.06
103.0	12.3	2.42
197.8	11.59	1.86

TABLE VII CONTINUED

RELATIVE QUANTUM YIELD OF PRODUCTS AS A FUNCTION OF

CARBON DIOXIDE PRESSURE

Mercury Droplet Temperature = 22°C, multiple reactor system*

Carbon Dioxide Pressure torr	Relative Yield of CO (g)	Relative Yield of Oxalate(s)	Total Yield
0.238	8.17	3.34	11.51
0.461	10.21	4.97	16.18
1.018	15.15	4.97	20.13
1.916	17.90	11.83	29.73
5.340	18.6	14.6	33.2
10.253	16.25	17.2	33.4
19.499	19.91	20.7	49.6

*See "Preface to the Description of the Kinetics of the Reaction" on page 52.

$$Hg6\ ^1P_1 + CO_2 \rightarrow HgOCO^* \qquad k_1(Hg6\ ^1P_1)\ (CO_2) \qquad (1)$$

Now let the excited complex decompose directly to yield carbon monoxide:

$$HgOCO^* \rightarrow HgO\ (s) + CO\ (g) \quad k_2(HgOCO^*). \qquad (2)$$

Let the excited complex also have a mode of decay to a triplet state which will form oxalate upon collision with carbon dioxide, and which otherwise is stable:

$$HgOCO^* \rightarrow HgOCO^3 \qquad k_3(HgOCO^*) \qquad (3)$$

$$HgOCO^3 + CO_2 \rightarrow HgC_2O_4 \qquad k_4(HgOCO)\ (CO_2) \qquad (4)$$

Now it has been shown that ultraviolet radiation decomposes oxalates of mercury:

$$h\nu + HgC_2O_4 \rightarrow Hg + 2CO_2 \qquad (5)$$

Also, it has been shown that oxalates of mercury easily pyrolyze:

$$HgC_2O_4 \rightarrow Hg + 2CO_2. \qquad (6)$$

According to this scheme, the relative rates of the production of CO (g) and solid oxalate is proportional only to (k_2/k_3). The appearance of the oxalate would also be dependent on the entire ultraviolet spectrum of the arc and the filter in any given run. The formation of oxalate, as the formation of carbon monoxide, would be dependent on carbon dioxide pressure only according to reaction (1).

If $HgOCO^3$ is relatively long lived (at least 10^{-6} seconds), the formation of oxalate from it will not appear to be dependent on the CO_2 pressure. Thus the true quantum yield is determined by the competing reactions

$$Hg6\ ^1P_1 + CO_2 \rightarrow HgOCO^* \qquad k_1(Hg6\ ^1P_1)\ (CO_2) \quad (1)$$

and

$$Hg6\ ^1P_1 \rightarrow Hg6\ ^1S_0 + h\nu \qquad 1/\tau(Hg6\ ^1P_1) \quad (7)$$

and it would be these reactions which would determine the inception of the plateaus described in Table VII and Figures 11 through 14. Were it not for the quantitatively unpredictable decomposition of the oxalate, the ratio of oxalate to carbon monoxide production would always be the same.

Lorentz broadening effects due to carbon dioxide pressure can also be considered. It is believed that these effects are negligible. This assumption is based on the fact that in the study of the reactions of $Hg6\ ^1P_1$ atoms with ethylene (41), the effect of increased ethylene pressure on increasing rate of product formation beyond the plateau region of quenching was not apparent; however, the addition of large amounts of xenon caused a marked increase in the relative quantum yield. This phenomenon may be attributed to Lorentz broadening of the mercury absorption, however, it will be shown in the mercury dependence study that the mercury vapor concentration was probably much higher than predicted by the slush bath temperature, due to the "virtual leak" of mercury atoms caused by adsorbed mercury atoms in the reaction system. This would give rise

to a very large amount of imprisonment of mercury radiation in the reactor (1), as well as increasing the extent of absorption of the tails of the absorption peaks, due to the kνNl relationship,where N is perhaps several hundred times larger than would be predicted by the slush bath temperature (at which KNl should be 2). These phenomena are believed responsible for the high percentage (95%) of reversible 1849A radiation measured for both types of resonance lamps. The increase in yield caused by xenon in the ethylene reactions may have been caused by the effect of xenon collisions with the suggested $Hg6\ ^1P_1\text{-}C_2H_4$ collision complex, these collisions altering the reaction coordinate or the lifetime of the complex.

Even if Lorentz broadening by xenon atoms is the cause of the increase of yield in the ethylene reaction, some parallel might be drawn between ethylene and carbon dioxide in their effects in Lorentz broadening if it is considered that their outmost electronic configurations are identical ($\pi^4 g$). Since ethylene pressure caused apparently little increase in yields due to Lorentz broadening, carbon dioxide would then probably not have either. The large number of vibrational and rotational modes in ethylene would make it even more likely to cause Lorentz broadening than CO_2.

FIGURE 15

PRODUCT RATES AS A FUNCTION OF TIME

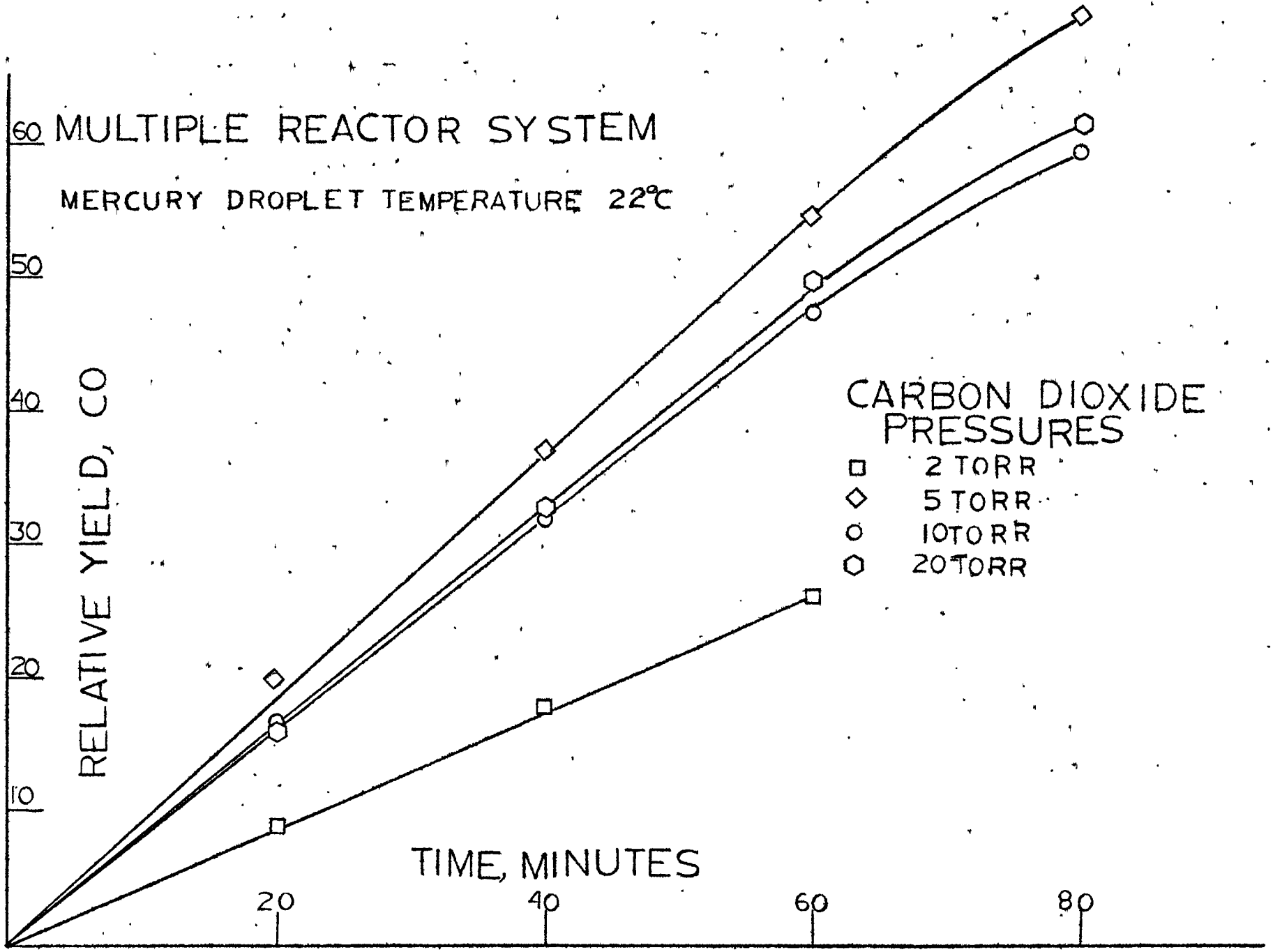
MULTIPLE REACTOR SYSTEM
MERCURY DROPLET TEMPERATURE 22°C
RELATIVE YIELD, CO
60
50
40
30
20
10
TIME, MINUTES
20
40
60
80
CARBON DIOXIDE PRESSURES
2 TORR
5 TORR
10 TORR
20 TORR

Effect of Reaction Time

The effect of reaction time is described in Table VIII and Figure 15.

TABLE VIII

RELATIVE YIELD OF PRODUCTS AS A FUNCTION OF TIME

Reaction Time (sec.)	Yield of CO (g)	Yield of Oxalate(s)
CO_2 Pressure 1.83 torr, multiple reactor system		
1200	8.77	2.66
2400	17.75	4.75
3600	25.7	5.94
4800	*	9.67
CO_2 Pressure 5.26 torr		
1200	19.9	4.23
2400	37.1	18.0
3600	54.5	25.0
4800	69.0	*
CO_2 Pressure 11.56 torr		
1210	16.82	12.5
2400	32.4	17.8
3590	47.4	22.3
4800	59.1	28.3

TABLE VIII CONTINUED

RELATIVE YIELD OF PRODUCTS AS A FUNCTION OF TIME

CO_2 Pressure 21.2 torr

Reaction Time (sec.)	Yield of CO (g)	Yield of Oxalate(s)
1200	13.5	1.53
2400	32.7	8.37
3600	51.8	19.1
4800	60.2	29.8

*These data were lost in analysis.

These data may be explained by assuming that the formation of products takes place as described in the previous sections, however, as the wall film begins to accumulate, the intensity of 1849A radiation entering the reactor becomes attenuated by absorption by the wall products, as depicted in Figure 15 by the tapering of the CO (g) production rate with increasing reaction time.

Effect of Mercury Vapor Pressure

The effect of mercury vapor pressure on the photosensitized decomposition of carbon dioxide is described by Table IX and Figure 16. (Table IX, page 70.)

The mercury vapor pressure was controlled by controlling the temperature of a drop of mercury in a cold trap. Various types of slush baths were used as constant temperature reservoirs. The

FIGURE 16

PRODUCT RATES AS A FUNCTION OF MERCURY PRESSURE

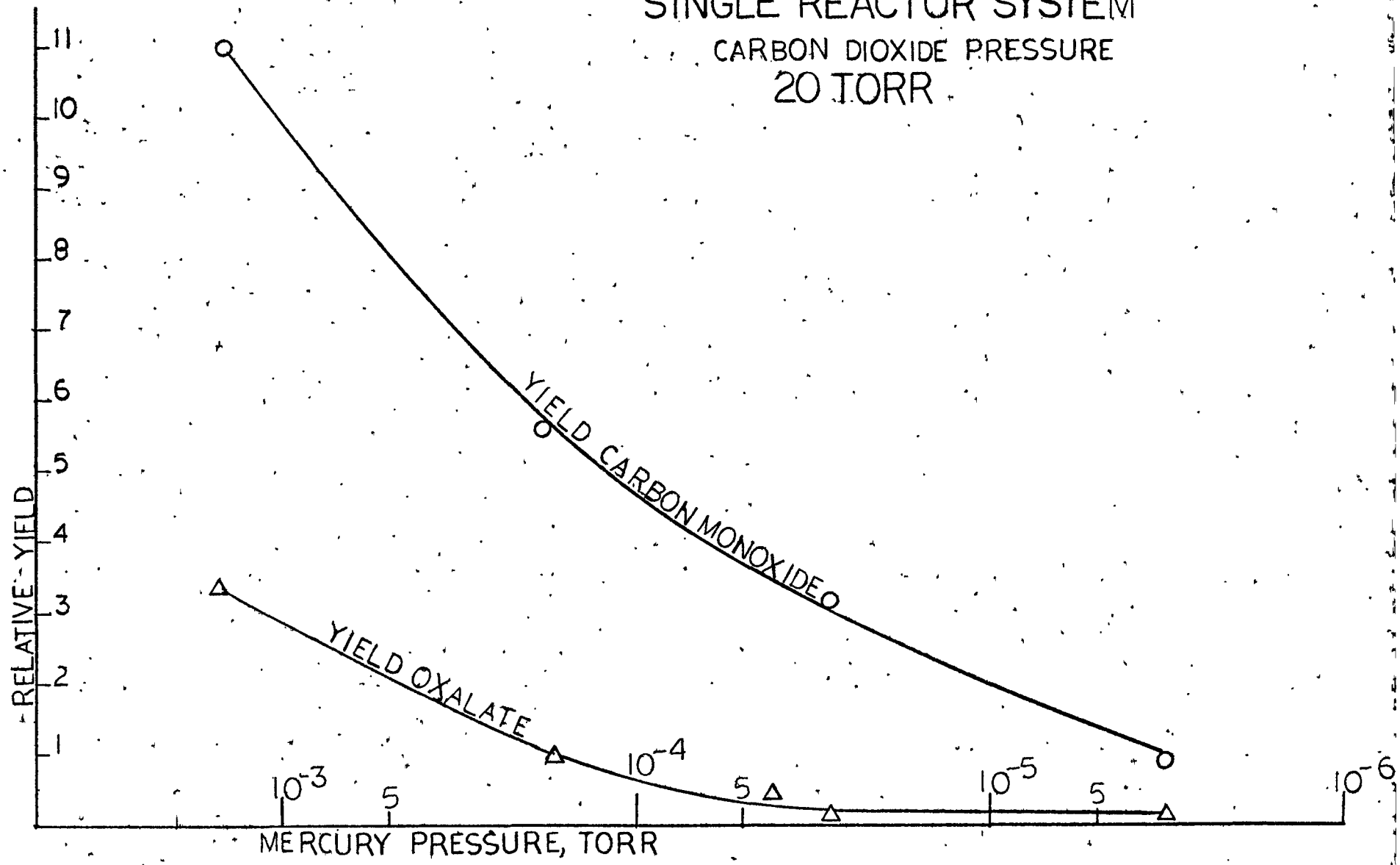
SINGLE REACTOR SYSTEM
CARBON DIOXIDE PRESSURE
20 TORR
RELATIVE YIELD
11
10
9
8
7
6
5
4
3
2
1
YIELD CARBON MONOXIDE
YIELD OXALATE
10^{-3}
5
10^{-4}
5
10^{-5}
5
10^{-6}
MERCURY PRESSURE, TORR

TABLE IX

YIELD OF PRODUCTS AS A FUNCTION OF MERCURY VAPOR PRESSURE

Carbon Dioxide Pressure 20 torr		Reaction Time 30 minutes	
Mercury Droplet Temperature	Mercury Vapor Pressure	Yield CO (g)	Yield Oxalate
22°C	1.44×10^{-3}	11.00	3.38
0°C	1.85×10^{-4}	5.60	0.99
-13.6°C	4.20×10^{-5}	*	0.40
-16.8°C	2.83×10^{-5}	3.18	0.13
-33.2°C	3.16×10^{-6}	0.84	0.14

*Products lost in analysis

reactant mixture was circulated through the entire reactor-cold trap loop in order to maintain the mercury vapor pressure as constant as possible.

Inspection of the data in Table IX and Figure 16 would readily lead one to believe that the reaction's mercury vapor pressure dependence is caused by the necessity of collision with the wall of an excited intermediate, since as the reaction is removed from the wall (by lowering the mercury vapor pressure), the yield sharply decreases. However, consideration of the first set of data in Table VII shows that the carbon dioxide pressure dependence of the reaction is roughly the same at low mercury vapor pressure as that at high mercury vapor pressures. If the reaction were truly wall dependent, the rate of product formation would become diffusion controlled at low mercury vapor pressure and would therefore become inversely proportional to the carbon dioxide pressure. Since this is not the case, the data may be explained by assuming that the mercury in the reaction mixture was consumed faster than it could be replenished, although considerable effort was made to keep the mixture sufficiently replenished with mercury. The explanation of the apparent non-variance of the reaction with very low mercury pressure lies in the fact that mercury adsorbed on the reaction loop's walls acted as a very low pressure virtual leak of mercury for the duration of the reaction. The fact that the deposits occurred heavily on the wall is explained by the fact the deposits were only large enough to be visible when the mercury

was at high pressures, and that at these high pressures most of the reaction took place within a few microns from the wall so that in this case deposit on the wall would be much more likely than sedimentation.

If the explanation of the mercury vapor pressure dependence data is valid, then the reaction mechanisms postulated in the previous sections are still plausible.

Several experiments were later conducted at very high carbon dioxide vapor pressure (253 torr), which in effect increases the number of collisions with CO_2 before striking the wall and thus would inhibit direct sedimentation on the walls. They were performed in a long tabular reactor which had a window sealed (with Apiezon wax) on one end of the tube and the other end was closed. The window in one case was γ-irradiated lithium fluoride wherein reactions were run at carbon dioxide pressures of 253 torr and 20 torr and with mercury vapor pressures corresponding to liquid at 22°C. In the other case a window of fused silica was employed under the same conditions. In both cases, the yellow (HgO) film did not appear on the window at high carbon dioxide pressure, but did appear at the low carbon dioxide pressures. In all four reactions, the gas phase product, when analyzed, was solely carbon monoxide. The geometry of the reaction systems employed in the kinetic experiments did not permit the distinction between film formation and sedimentation of the solid products.

The experimental details of the work just discussed shall be described in the following section. Thereafter, the results of the research shall be summarized and conclusions drawn from them.

Experimental

This section will first describe the apparatus and procedure employed in the research and then describe the details of the more important experiments.

General Vacuum System

This is a typical vacuum system for the manipulation of volatile inorganic compounds. Greased stopcocks were employed since none of the gases of concern (oxygen, carbon monoxide, and carbon dioxide) were seriously affected by stopcock grease (which was Apiezon L and Apiezon N) (4). This system is diagrammed in Figure 17. The system was capable of achieving a sticky vacuum (pressure at and below where the mercury thread in the McLeod gauge sticks to the top of the capillary upon pressure measurement) to atmospheric pressure in less than an hour. The McLeod gauge could distinguish 10^{-6} torr from sticky vacuum. The pressure rise in the high vacuum portion from sticky vacuum overnight was on the order of 10^{-5} to 10^{-4} torr.

The system was serviced periodically by cleaning the large removable traps, regreasing the stopcocks and joints, and scrubbing under vacuum with a Tesla high voltage discharge.

The manometer was read with either of two cathetometers, one for large pressure measurement, with a precision of 0.1 millimeter, and the other for measurement of smaller pressures, with a precision of 0.001 millimeter.

FIGURE 17

GENERAL VACUUM SYSTEM

Legend:

A Mechanical roughing pump

B "Bleeder" inlet

C Cold trap

D Mercury diffusion pump

E Distillation trap

F "K" bottle of CO_2

G Rubber vacuum tube

H Multiple Reactor System, Service Manifold

I McLeod gauge

J Manometer

K Reservoir, 2 liter

L Inlet to reactor system

M Auxiliary inlet

X2 Stopcock, 2mm bore

X4 Stopcock, 4mm bore

X6, Stopcock, 6 mm bore

X10, Stopcock, 10 mm bore

Taper joint, S 10/30, male, ground

Taper joint, S 10/30, female, ground

Ball joint, S 12/5, ground

Ball joint, S 18/9, ground

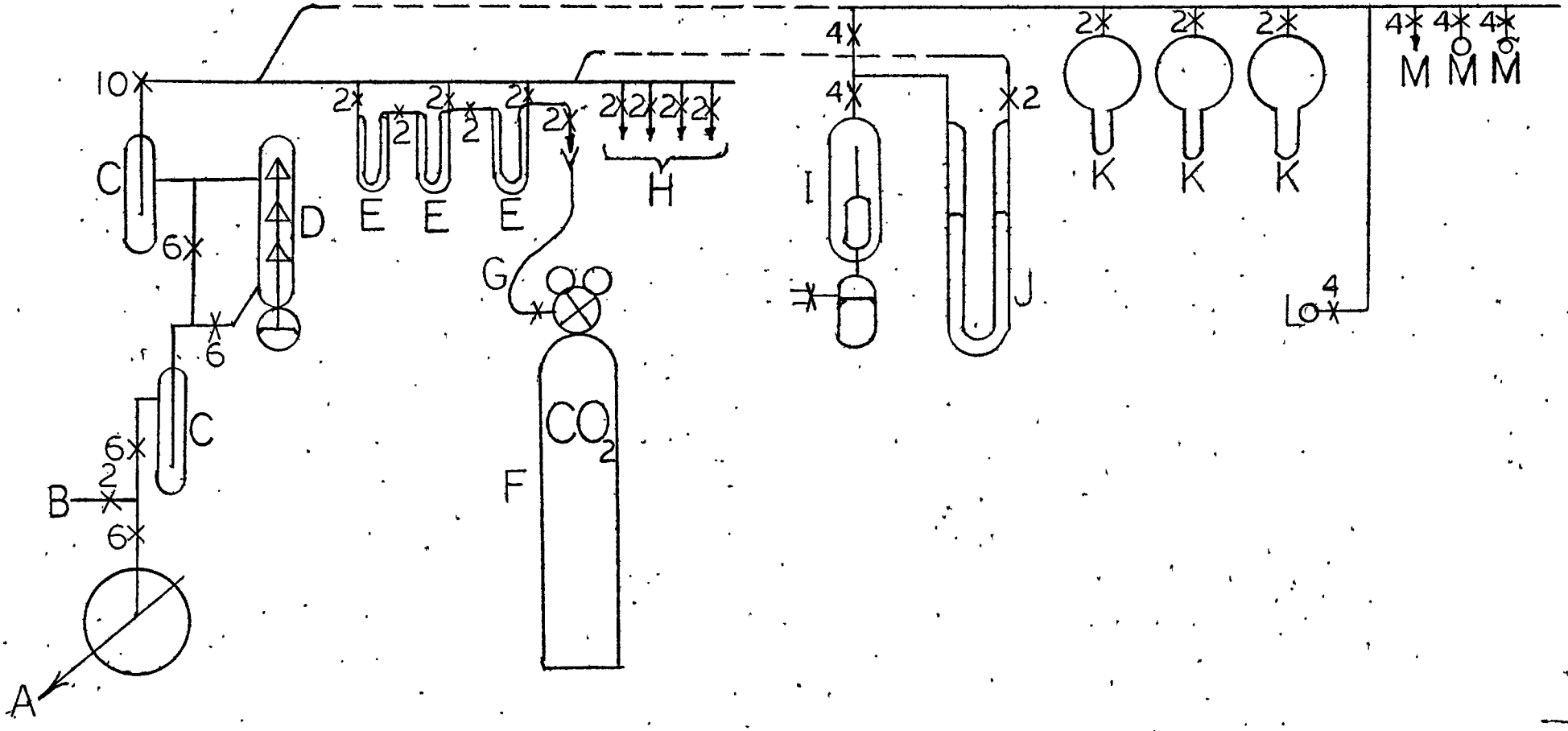
10
C
6
D
6
C
6
2
B
6
A
2
E
2
E
2
E
2
H
G
F
CO_2
4
4
2
I
J
2
2
K
2
K
2
K
4
M
4
M
4
M
4
Lo

The McLeod gauge was calibrated against this laboratory's standard McLeod gauge by measurement of common pressures. This standard was calibrated by Professor Richard Pertel by the method of measuring the volume of the reservoir and capillaries, and the cross sectional areas of the capillaries directly by measuring the weight and length of mercury required to fill them. The McLeod gauge had one quadratic scale of 100 to 10 microns, one quadratic scale of 10 microns to sticky vacuum, and one linear scale of zero to 2 torr.

Purification and Storage of Carbon Dioxide

The carbon dioxide reactant gas was obtained from a "K" bottle containing Matheson purified carbon dioxide (99.95% minimum purity). The main caution taken in transferring the carbon dioxide into the vacuum system was to prevent moisture and air from contaminating the gas. Moisture quenches Hg6 $^1P_1$ atoms severely and the presence of air would give spurious results in the manometric analysis of the products. A vacuum connection was made from the pressure regulator on the "K" bottle to the vacuum system. This system was evacuated, filled with carbon dioxide, and re-evacuated. Carbon dioxide was then admitted to the system at a pressure of 760 torr and the system, excluding the extra apparatus for transfer of CO_2, was sealed. A Dewar flask containing a dry ice-acetone bath (-78.5°C) was placed about a cold trap in the distillation train (the vapor pressure of ice at -78.5°C is 0.52 microns Hg) in order to remove the water. The trap was sealed off after an hour of exposure. The air was removed by thrice repeated

condensation and sublimation with liquid nitrogen about the cold finger of the two liter reservoir that will store the CO_2. After each condensation the system containing the solid carbon dioxide was pumped to sticky vacuum. The vapor pressure of solid carbon dioxide at 77°K is less than 10^{-7} torr. (43). After the pressure of CO_2 reached approximately five torr on sublimation the reservoir containing the CO_2 was sealed off and this portion was evacuated. Before carbon dioxide was delivered to the reactor it was condensed by liquid nitrogen, pumped down to sticky vacuum, the system sealed, and the carbon dioxide allowed to sublime to the desired reactant pressure, as monitored by either the manometer or McLeod gauge.

Gas Chromatograph Doser

A device was necessary for transferring the very small quantities of reaction products (as small as 0.1 micromole, near 1 micron pressure) into the chromatograph system for analysis with the admission of no greater than 0.01 micromole of air into the system. An all-glass system was designed for this purpose and is depicted in Figure 18. The doser is simply a mercury piston, modeled after a Topler pump. The sample is transferred into the dosing chamber, sealed, and another portion of gas is brought up to the dosing chamber, the chamber opened, and the new sample is collected with that of the previous stroke. The amount of sample collected increases asymptotically with the number of strokes. A practical number of strokes was six. After the sixth stroke, the dosing chamber was again sealed off from the piston chamber

FIGURE 18

GAS CHROMATOGRAPH DOSER

Legend:

A Vacuum, lowering piston

B Air, raising piston

C Ground socket joint, S 18/9, to reactor system

D Vacuum stopcock, 4 mm bore

E Mercury reservoir

F Collecting chamber

G High pressure stopcock, 2 mm bore

H High pressure stopcock, 120°-3-way, 2 mm bore

I Carrier gas inlet

J Carrier gas outlet, to column

K Evacuation outlet

L Dosing chamber

GAS CHROMATOGRAPH DOSER

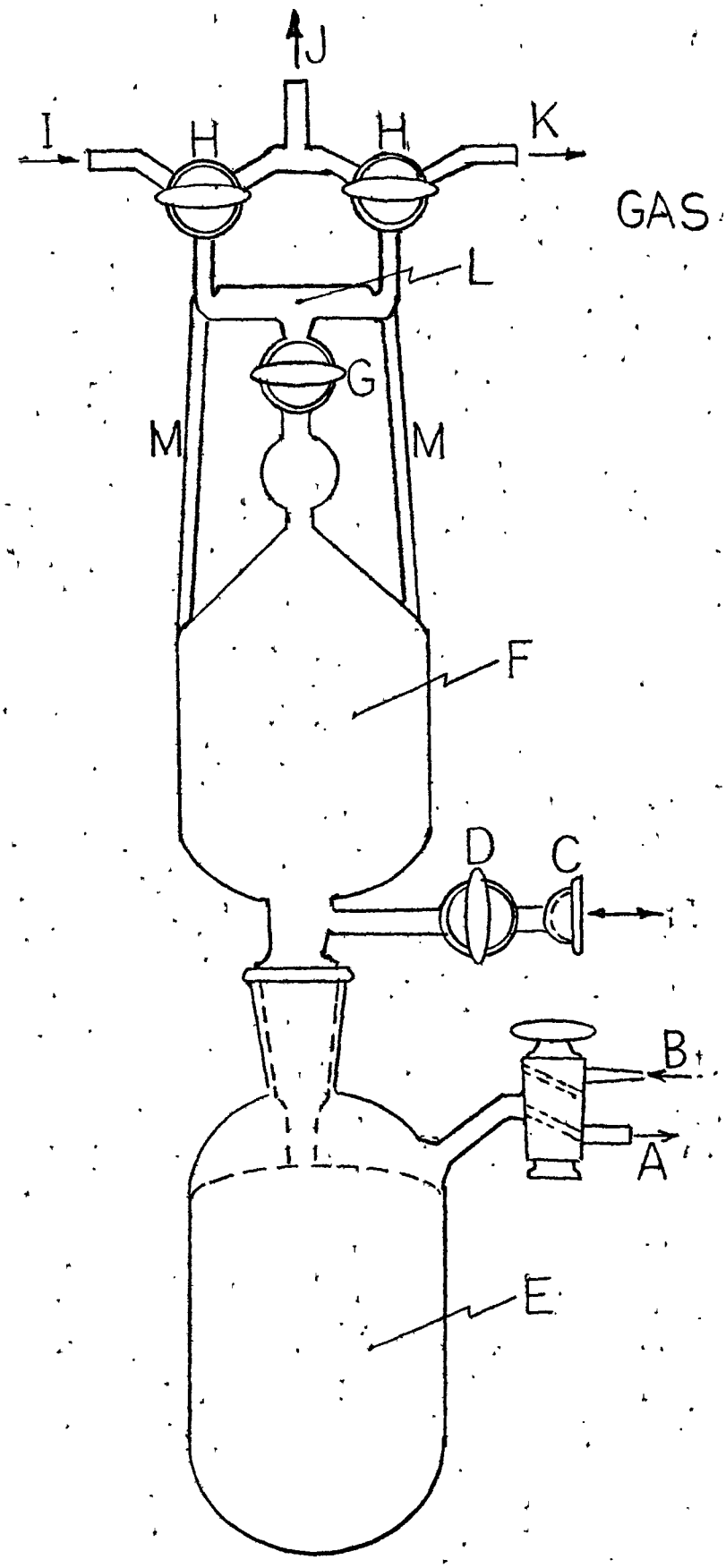

and the gas chromatograph stream was diverted through the dosing chamber, sending the sample on to the gas chromatograph column. The doser, including dosing chamber, is evacuated to sticky vacuum before each application.

Reaction System

The filter system and light sources employed in the reaction system have been described in Section II.

Three reaction systems were employed. The first reactor consisted of a circulation system, spiral electroded lamp, and tubular reactor, with the annular filter jacket around the reactor and inside the lamp's spiral. This system was used to obtain products for the qualitative analyses. It is depicted in Figure 19. The second reaction system consisted of the circulation system, the electrodeless mercury arc, and an annular reactor. The lamp was inside the filter jacket, the jacket being inside the annulus of the reactor. This second reaction system was used in the kinetic studies involving the carbon dioxide pressure dependence at high and low mercury pressures and the effect of the intensity of 1849A radiation dependence as well as in several special experiments. This system, depicted in Figure 20, has been called the "single reactor" system since only one data point per lamp ignition could be obtained from it. The purpose of the reservoir is simply to act as a ballast. Before each run, in either of the first two systems, the entire reaction system was scrubbed under vacuum with a Tessla coil and the reactor was then flamed under vacuum to incipient

FIGURE 19

REACTION SYSTEM FOR QUALITATIVE DATA

Legend:

A Suprasil reactor

B Suprasil filter jacket

C Connection to filter circulation system

D Cold trap

E Mercury droplet

F Circulation pump

G Solenoid

H Pyrex encased plunger

I Connection to Gas Chromatograph Doser

J Connection to General Vacuum System

K Section of circulation system

N N_2 purge inlet

P Cardboard enclosure (top and bottom sealed)

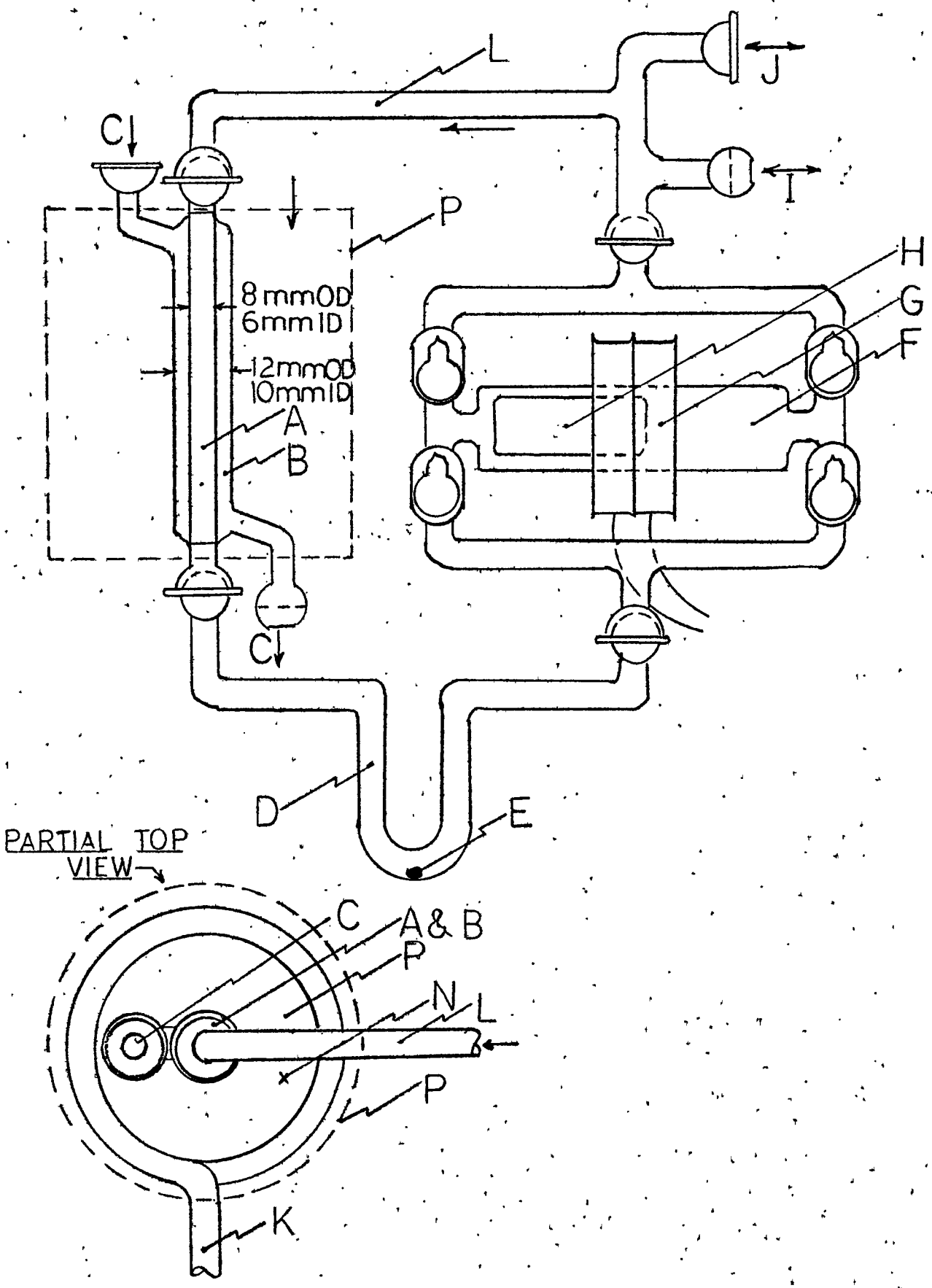

REACTION SYSTEM FOR QUALITATIVE DATA

FIGURE 20

SINGLE REACTOR SYSTEM

Legend:

A Cooling water inlet

B Connection to filter circulation system

C Electrodeless arc

D Reactor, internal optical path 7 mm

E Filter jacket

F Ballast, 2 liter

G Mercury droplet

H Circulation pump (see Figure 15)

I Connection to Gas Chromatograph Doser

J Connection to General Vacuum System

N Nitrogen purge inlets

SINGLE REACTOR SYSTEM

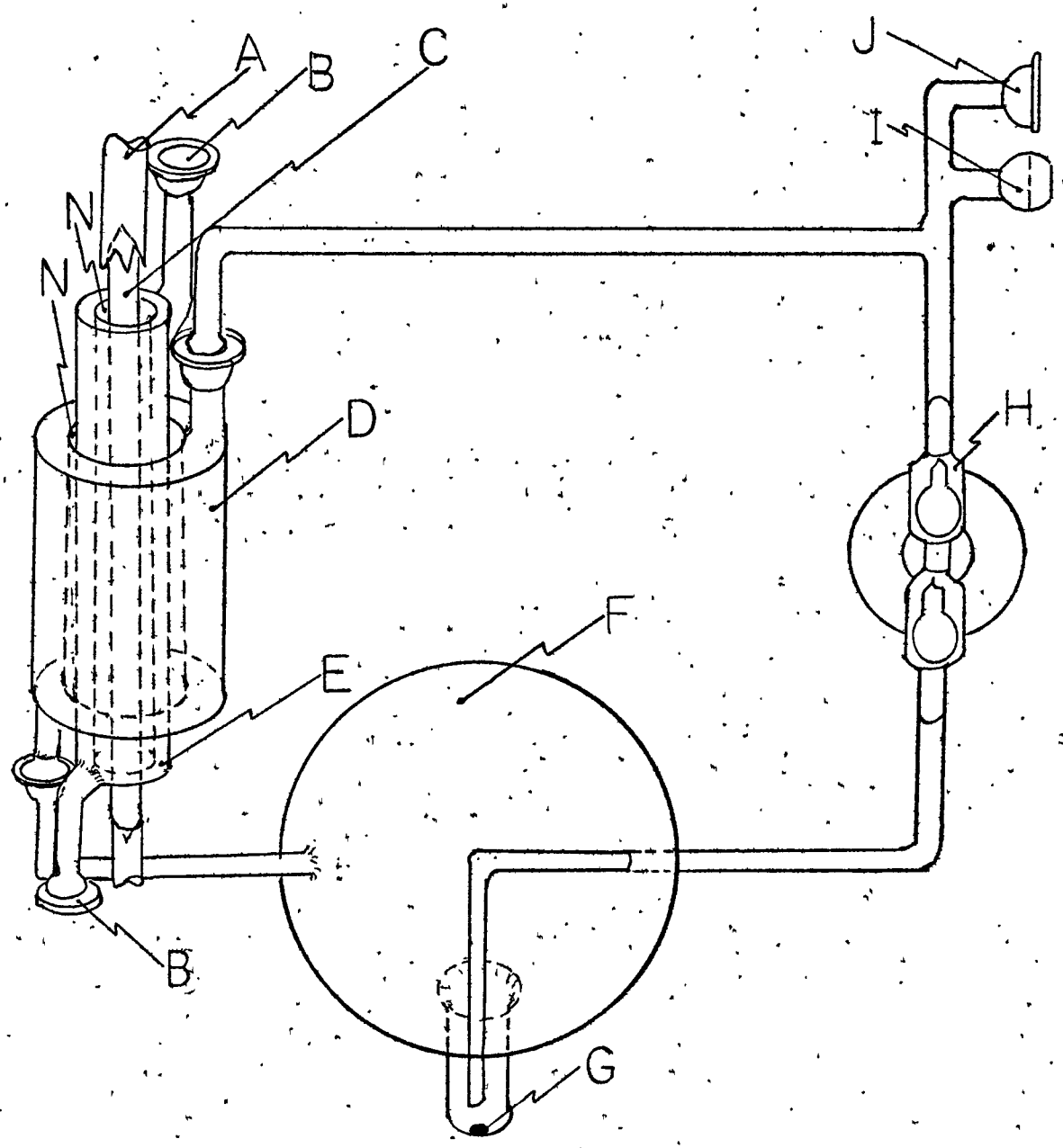

red heat. After carbon dioxide reactant gas was admitted to the reaction system, the gas was precirculated (before lamp ignition) for at least thirty minutes so that all of the mercury in the gas of the system could come into equilibrium with the droplet of mercury in the cold finger of the reservoir.

The third reaction system was employed in the study of the time dependence and carbon dioxide pressure dependence of the reaction at high mercury vapor pressures (corresponding to a mercury droplet temperature of 22°C).

This reaction system, previously mentioned as the "multiple reactor" system, permitted the taking of four data points during a single lamp ignition; e.g., four pressures or four different exposure times. The four reactors were then placed on the vacuum system on the manifold provided for them (see Figure 17), evacuated, flamed and scrubbed with the Tessla coil. Then they were filled with carbon dioxide, each one to the desired pressure, sealed via their individual stopcocks and removed from the reaction system and placed in the resonant microwave cavity. The composite system is depicted in Figure 21. After exposure the reactors were returned to their manifold on the vacuum system and each individually analyzed. This system was designed to overcome the problems in data taking caused by inconsistencies in the lamp from ignition to ignition. In order to adjust for inhomogeneities in the four reactors, a run was made with all four reactors filled at the same carbon dioxide pressure (20 torr) and all were exposed in the same time period (30 minutes). The amount

FIGURE 21

MULTIPLE REACTOR SYSTEM

Legend:

A Reactor (Pyrex reservoir indicated)

B Suprasil tubing

C Vacuum stopcock, 2 mm bore

D Pyrex-Vycor graded seal

E Filter jacket

F Connection to filter circulation system

G Electrodeless arc

H Cooling water inlet

I Plastic cover

J Microwave antenna

K Mercury droplet

L Ground glass joint (S=12/30)

MULTIPLE
REACTOR
SYSTEM

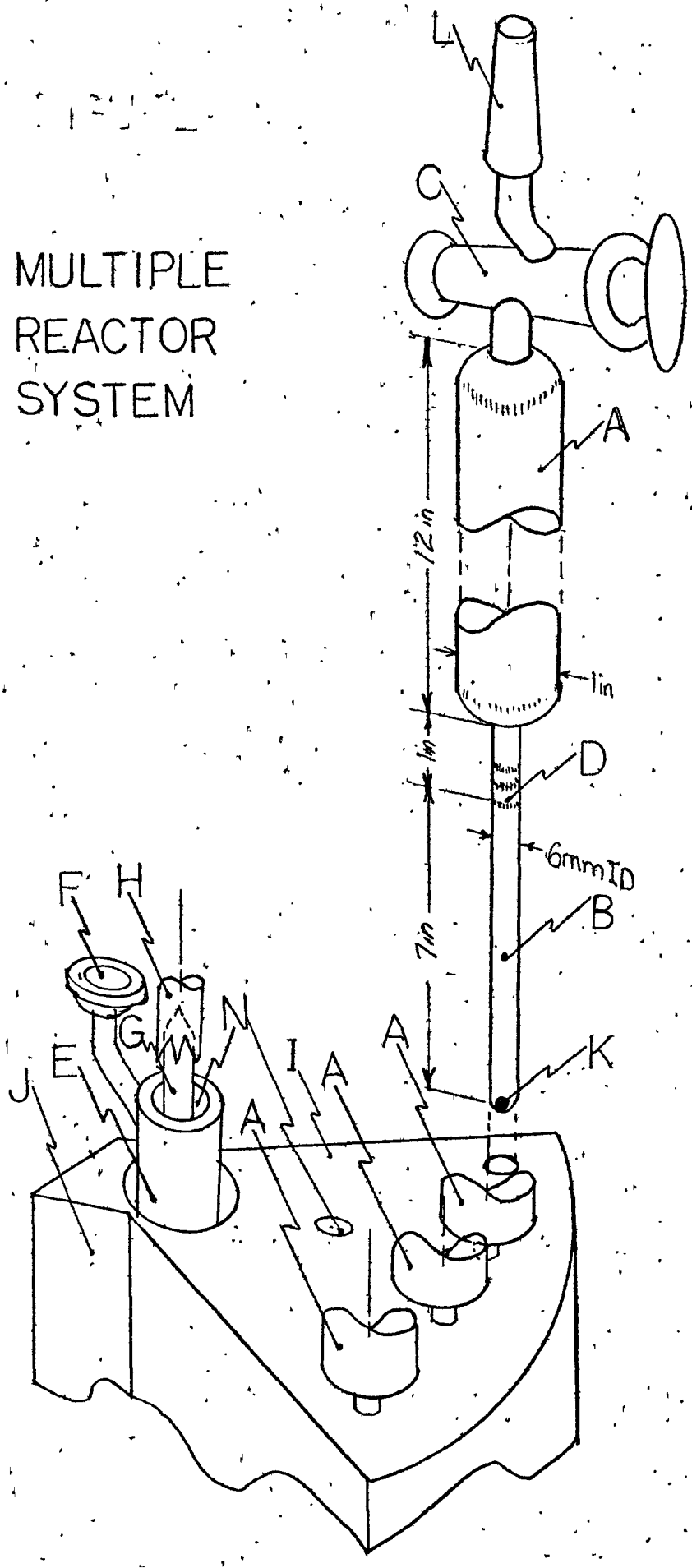

of products was very nearly the same in all four reactors, but their differences were noted and a normalization factor for the CO(g) yield and for the oxalate(s) yield of each reactor was calculated for the normalization of the results of each set of data from the four reactors. The yield of a reactor, multiplied by its corresponding normalization factor, gave the normalized yield. The yields and respective normalization factors are listed in Table X.

TABLE X

NORMALIZATION FACTORS FOR MULTIPLE REACTOR SYSTEM

CO_2 Pressure = 20 torr, Time = 30 minutes, Mercury droplets at 22°C

Reactor Number	Yield of Co(g)	Yield of Oxalate as CO_2(g) (Microns Mercury)	Factor for CO(g)	Factor for Oxalate
1	1.06	0.60	1.180	0.867
2	1.25	0.53	1.000	1.000
3	1.31	0.53	0.954	1.000
4	1.22	0.53	1.025	1.036

Reactor #2 was taken as reference.

All of the reactors described in this section, the filter jacket, and the electrodeless lamps were boiled in a mixture of concentrated nitric acid and sulfuric acid after every four or five runs. They were rinsed with distilled water and alcohol. In every run a nitrogen

purge was placed in the annular spaces or cavities in order to remove the 1849Å absorbing oxygen from the optical path. All non-enclosed quartz surfaces and the filter system was rinsed or washed with alcohol before each run. The reactions were timed with an electric timer whose precision was 0.1 second.

Gas Chromatograph System

The gas chromatograph system consisted of the doser (see Figure 18), carrier gas source, column, detector, power supply, amplifier, and recorder as depicted schematically in Figure 22.

The column selection was originally silica gel-iodine pentoxide-silica gel (44). A ten foot spiral glass column contained equal lengths of silica gel separated by a three inch section of iodine pentoxide (anhydrous). The column was wrapped in aluminum foil, then wrapped with a heating tape, placed in a coffee can and insulated with glass wool, and maintained at 115°C. The first portion of the silica gel separated air and carbon monoxide from carbon dioxide, the iodine pentoxide converted the carbon monoxide to carbon dioxide and the latter section of silica gel separated the converted carbon dioxide from air, thus overall separating air, carbon monoxide, and carbon dioxide. The carrier gas used for this column was helium doped with 5% methane. The column performed well when fresh but became erratic with use, and was thus rejected. The chromatographic columns' resolutions were measured with gas mixtures (air, O_2, CO, and CO_2) prepared in and transferred

FIGURE 22

GAS CHROMATOGRAPH SYSTEM

Legend:

A Carrier gas source

B Gas Chromatograph Doser (see Figure 18)

C Chromatographic column

D Detector (cross section)

E Power supply

F "Buckout" current source

G Picoammeter

H Strip chart recorder without disc integrator

GAS CHROMATOGRAPH SYSTEM

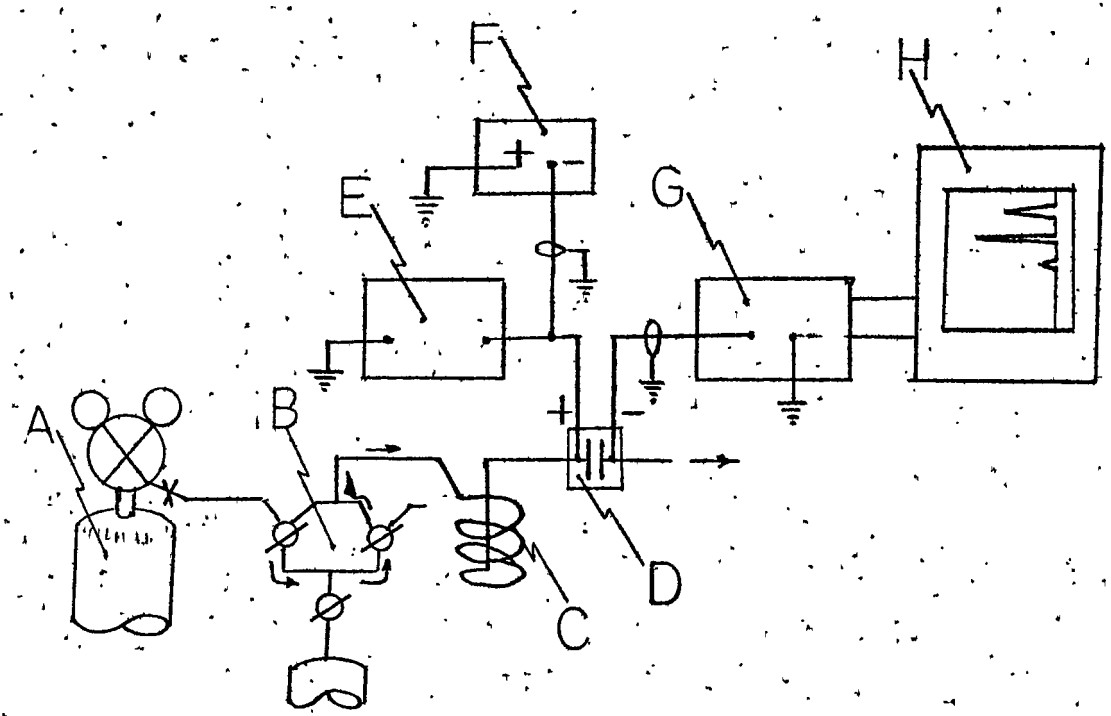

from the vacuum system. When it became apparent that the analysis of the kinetic runs only required verification of the gas phase non-condensable product as CO, a 20 foot long column filled with activated charcoal (45) and using hydrogen as carrier was employed. The column was flamed before each usage to assure high activation of the charcoal. The column was used at room temperature. The column was often checked for resolution of air and carbon monoxide and was always found reliable. The column separated air from carbon monoxide very well and resolved nitrogen and oxygen well enough that either gas was clearly distinguishable (see Figure 23). When it became necessary to identify carbon dioxide as in the pyrolysis of the film, a three foot silica gel column (46), using hydrogen as carrier, was employed at room temperature. The column was reliable and gave good separation of carbon dioxide and air.

Analysis of Products in Kinetic Runs

The identity of the gas phase product as solely carbon monoxide was established by chromatography using both the silica gel and the charcoal columns. The silica gel column verified that only permanent gases were present in the product mixture, other than carbon dioxide. The charcoal column verified that no oxygen was present even at low mercury vapor pressures.

The reactor's pyrolysis products were identified as carbon dioxide and permanent gas by the silica gel column, and the permanent gases were identified as solely oxygen by the charcoal column.

FIGURE 23

TYPICAL CHROMATOGRAM

CHARCOAL COLUMN, H_2 CARRIER

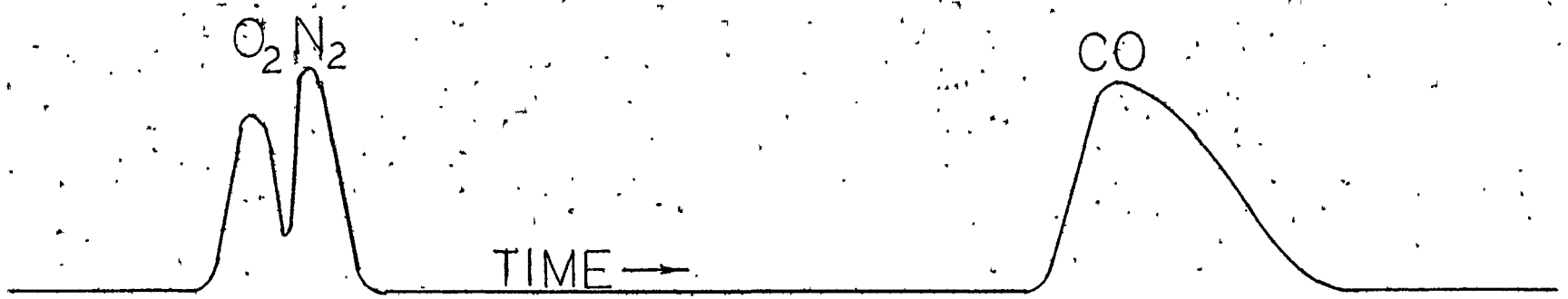

With this composition, the products became analyzable by simple manometric methods. The kinetic runs were analyzed by first condensing the remaining reagent carbon dioxide with liquid nitrogen and measuring the pressure of the residual non-condensable gases. Pure reagent carbon dioxide was measured this way and the residuals were in the range of 10^{-5} torr. The smallest non-condensable product gas pressure measured was greater than 10^{-4} torr. It will also be recalled that the vapor pressure of carbon dioxide at liquid nitrogen temperature is less than 10^{-7} torr. After the gas phase product (CO) was analyzed, all of the gas phase reaction mixture was pumped away (to sticky vacuum) and the reactor was sealed and pyrolyzed to incipient red heat with a natural gas-oxygen torch. After the reactor cooled, the pressure of the gaseous products resulting from the pyrolysis was measured manometrically. The carbon dioxide in the gas mixture resulting from film pyrolysis was removed by the liquid nitrogen cooling of a cold trap (refer to Figure 17), and the residual, non-condensable gas pressure was measured as oxygen. Several checks with the charcoal chromatographic column verified that this gas was truly oxygen.

The volume of the measurement system was determined manometrically, using one of the large reservoirs, whose volume was determined by the weight of water it contained, as a reference. This volume was 1.281 liters. The number "11.00" mentioned as CO(g) product in the kinetic runs using the "single reactor" system (see Tables VI and VII), which is representative of the yield in the plateau region of carbon dioxide

pressure for a 30 minute run at room temperature mercury droplet, corresponds to about 1.73 micromoles of carbon monoxide. The number 11.00 is the hourly yield in moles of CO(g) product divided by the filter's 1849A transmission and multiplied by 10^5. Therefore, a CO(g) yield of 11.00 means there would be 11.00 x 10^{-5} moles of carbon monoxide produced per hour if there were no filter.

Analysis of Oxalate by the Diphenylamine Test

The test, as prescribed by Feigl (38), can distinguish oxalate from carbonate, formate, acetate, and other organic acid anions in the manner it is herein conducted.

Carbon dioxide at 37.1 torr was decomposed by photosensitization with Hg6 $^1P_1$ atoms in the absence of Hg6 $^3P_1$ atoms (with a filter) for twenty minutes at a mercury vapor pressure corresponding to room temperature mercury droplet. The reaction system was of the first type, i.e., the spiral lamp and tubular reactor. After the reaction, the film was washed from the reactor with a few ml of 1.5N HCl. The solution was evaporated in a test tube down to 1/2 ml, decomposing any carbonic acid that may have been formed if $HgCO_3$ were present. A few crystals of reagent grade diphenylamine were added and heating of the test tube continued. A blue colored solution resulted (the positive test for oxalate). This solution was diluted in ethanol and its transmission spectrum was measured. This procedure was repeated using 1.5N HCl solutions of oxalic acid and of various quantities of mercuric oxide which also was present in the reactor. The results are listed in Table XI.

TABLE XI

RESULTS OF DIPHENYLAMINE TEST FOR OXALATE

Sample	Spectrum
Unknown	Medium absorption peak at 610 mμ
Oxalic Acid	Strong absorption peak at 610 mμ
Relatively large amount of HgO	Medium absorption peak at 610 mμ
Smaller amounts of HgO, but still larger than that present in reactor	Very weak absorption peak at 610 mμ

It is concluded that the film very likely contained an oxalate.

Analysis of Oxalate by Decoloration of Potassium Permanganate

The reactor of a typical kinetic run ("single reactor" system) was washed with dilute HCl and the solution was transferred to a test tube. Three other test tubes were filled with the same acid; one contained a small amount of mercuric oxide, one contained a small amount of mercuric oxalate, and one was empty. Two drops of thioacetamide were added to each test tube. The solutions were then boiled, centrifuged, boiled, and centrifuged again. The supernatant solutions were added to four respective Erlenmeyer flasks containing equal aliquots of very dilute $KMnO_4$. The visible transmission spectrum of each

solution was measured as well as visually inspected. In both tests the sample from the unknown film of the reaction and the sample from the mercuric oxalate decolored the permanganate.

It is concluded that the film product very probably contained oxalate.

Decomposition of Mercury Oxalates

Mercuric Oxalate

Mercuric oxalate was freshly prepared by mixing slowly and with stirring a solution of oxalic acid and one of mercuric acetate, respectively. The very finely powdered product was washed several times with ethanol and dried in a vacuum desiccator. A sample was weighed out (0.1249 gm) and was placed in the reaction system described in Figure 24. It was then evaculated to sticky vacuum and exposed to irradiation from the spiral electroded lamp.

Results: The pressure in the system rose from sticky vacuum to 3.0 torr. The gas phase products were subjected to liquid nitrogen temperature via a cold trap and the pressure of the residual non-condensable gas was 76 microns. This was analyzed with a charcoal gas chromatographic column to be only carbon monoxide.

There was a greyish yellow coating on the oxalate in the suprasil quartz portion of the reactor (which transmits resonance radiation), and on the suprasil; whereas the oxalate in the 7913 vycor glass section (which did not transmit resonance radiation) had only a grayish black coating, which was also present in the suprasil side, but no

FIGURE 24

REACTOR FOR DECOMPOSITION OF OXALATES

Legend:

A Suprasil portion

B Vycor 7913 portion

C Oxalate

D Vycor ℠ 12/5 balljoint

E Pyrex cold trap

F Connection to general vacuum system

REACTOR FOR DECOMPOSITION OF OXALATES

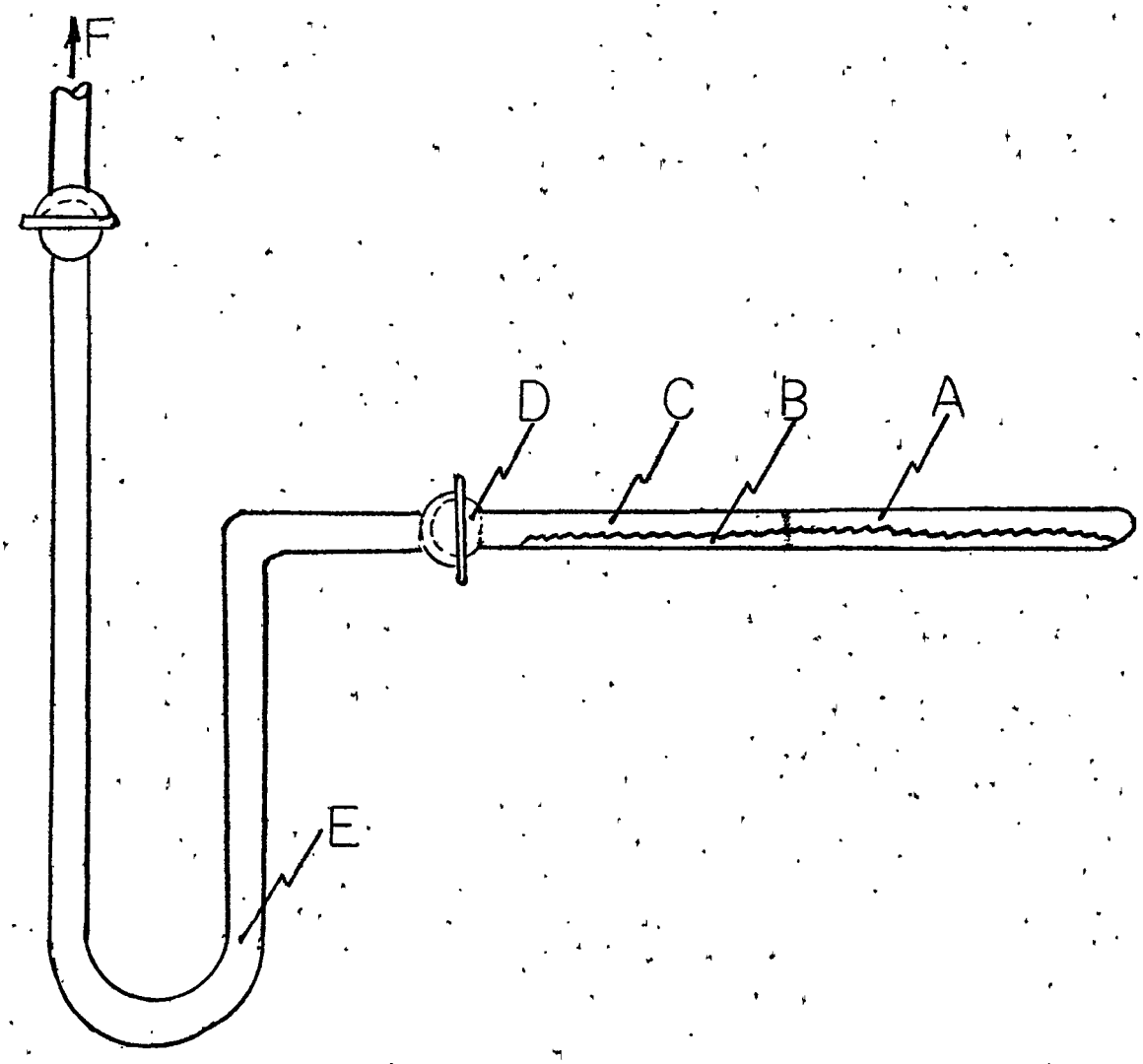

yellowish coating appeared on the vycor wall or on the oxalate in the vycor section.

The system was evacuated and the remaining mixture was partially pyrolyzed with a heat gun (approximately 250°C). The pressure rose from sticky vacuum to 35.2 torr. The gaseous products were then subjected to liquid nitrogen temperature and the pressures of the non-condensable gas (with the McLeod gauge now open) was 90 microns. This gas was analyzed by the charcoal chromatograph column to be composed of only carbon monoxide. The oxalate in the vycor portion still did not turn yellow, and only a silvery mercury deposit was found on the reactor wall. Further decomposition with a natural gas-oxygen torch also did not cause any yellow film on the oxalate in the vycor section or on the vycor wall.

Conclusions: The yellow film is assumed to be mercuric oxide. The condensable gas is assumed to be carbon dioxide. If so, the mercuric oxalate photolytically decomposes as follows:

$$HgC_2O_4 + h\nu \text{ (1849A to 2600A)} \rightarrow Hg + 2CO_2,$$

also, $$HgC_2O_4 + Hg6\ ^3P_1 \text{ and/or } Hg6\ ^1P_1 \rightarrow 2Hg + 2CO_2.$$

A secondary reaction occurs when the carbon dioxide product pressure gets sufficiently high:

$$Hg6\ ^1P_1 + CO_2 \rightarrow HgO + CO$$

as evidenced by the coating of mercuric oxide on the upper walls of

the suprasil section of the reactor and by the presence of carbon monoxide in relatively small amounts.

The HgC_2O_4 is pyrolyzed at heat gun temperatures by the mechanism:

$$HgC_2O_4 \rightarrow Hg + 2CO_2.$$

It decomposes similarly at higher temperatures (i.e., flaming the reactor with the gas-oxygen torch). The trace of CO (<0.1%) may be produced by a much less favored pyrolysis mechanism.

Mercurous Oxalate

Mercurous oxalate ($Hg_2C_2O_4$) was prepared by adding solid mercurous nitrate, with vigorous stirring, to a boiling solution of oxalic acid. The precipitate was washed with hot water, ethanol, and ether. It was then dried in a vacuum desiccator. The mercurous oxalate was photodecomposed and then pyrolyzed in the same apparatus and in the same manner as was the mercuric oxalate.

Results: The pressure after photodecomposition rose from sticky vacuum to 1.89 torr. The "non-condensable" gases analyzed by the charcoal chromatograph column to be only carbon monoxide were at a pressure of 0.1828 torr. The suprasil quartz section's wall had a heavy silvery yellow mirror, which was visibly absent on the reactor wall in the vycor portion. The solid in the vycor section was white with a black coating over about 75% of its surface. The solid in the suprasil section had a more yellowish-white appearance, but also had a gray-black coating. The pyrolysis products were again mainly carbon dioxide with a small amount of carbon monoxide.

Conclusions: The mercurous oxalate photodecomposes and pyrolyzes in the same manner as mercuric oxalate.

TABLE XII

SUMMARY OF RESULTS OF DECOMPOSITION OF OXALATES OF MERCURY

Compound	Ratio of CO/CO Photolysis	Ratio of CO/CO Pyrolysis
Mercurous Oxalate	0.0966	0.01162
Mercuric Oxalate	0.0258	0.00373

The amount of carbon dioxide analyzed in the film pyrolysis of the Hg6 $^1P_1$ + CO_2 reaction was so small that a few percent of carbon monoxide, if present, could not be detected. It is also shown here that mercury oxalates decompose mainly into mercury and carbon dioxide at wavelengths above, and of course, below, the cut-off of 7913 vycor glass, which is about 2600A.

Determination of the Mechanism of Formation of Mercuric Oxide

The object of this experiment is to determine whether free oxygen is produced by the Hg6 $^1P_1$ + CO_2 reaction and scavenged by mercury vapor to form mercuric oxide, or if mercuric oxide is formed as a direct product of decomposition of the Hg6 $^1P_1$ + CO_2 collision complex.

The answer can be found by lowering the mercury vapor pressure from a few microns (room temperature liquid) to less than 10^{-5} torr (tetralin slush bath temperature liquid), making collisions between oxygen atoms and mercury atoms highly improbable, and thus favoring collisions between oxygen atoms to form molecular oxygen.

The "single reactor" system was used with filter. The carbon dioxide pressure was 20.1 torr and the exposure was quite long, two and a half hours, in order that sufficient products could be produced for chromatographic analysis. The mercury droplet was maintained at -33°C using a tetralin slush bath.

Results: The gas chromatogram, using the charcoal column, showed that if molecular oxygen was formed, its concentration was less than 0.1% of the carbon monoxide concentration.

Conclusion: No atomic oxygen is formed in the Hg6 $^1P_1$-CO_2 reaction. If a Hg-O-CO complex is formed, it decomposes directly into mercuric oxide and carbon monoxide.

Photodecomposition of Solid Product from the Hg6 $^1P_1$ Photosensitized Decomposition of Carbon Dioxide

The object of this experiment is to determine the mode of photodecomposition of the solid (wall) product of the Hg6 $^1P_1$ + CO_2 reaction and to compare it to the mode of photodecomposition of the oxalates of mercury.

Carbon dioxide at 18.9 torr was reacted in a "single reactor" apparatus for 80 minutes, using a filter. The gaseous component was

then evacuated, the reactor sealed and photolyzed for 50 minutes. The gas phase products of the film photolysis were then analyzed manometrically and also by chromatography. These products were evacuated, the reactor again sealed, and the remaining film was pyrolyzed with a gas-oxygen torch. The pyrolysis products were also analyzed monometrically and by gas chromatography. The entire experiment was then repeated, except that the film formation reaction lasted 205 minutes and the film photolysis reaction lasted 85 minutes.

Results: The photolysis products from the first reaction were analyzed as carbon monoxide and carbon dioxide. The ratio of CO_2/CO in this reaction was 0.21. The film pyrolysis products were oxygen and carbon dioxide; the CO_2/O_2 ratio was 0.915.

The photolysis product from the second reaction (longer photolysis time) was only carbon monoxide. The pyrolysis products were carbon dioxide and oxygen, the CO_2/O_2 ratio being 0.782.

The yellow film persisted after photolysis, but disappeared upon pyrolysis, in both runs.

Conclusions: The disappearance of carbon dioxide in the extended photolysis indicates that the solid $Hg6\ ^1P_1 + CO_2$ reaction product decomposes first into carbon dioxide, which then is decomposed by $Hg6\ ^1P_1$ atoms to carbon monoxide. It is recalled that this is the same behavior of mercury oxalates on photolysis. The production of carbon dioxide in the pyrolysis can be attributed to oxalate pyrolysis, and the disappearance of the yellow film and the formation of oxygen in the pyrolysis indicates that this film was mercuric oxide.

Thus, the wall products are very likely mercuric oxide and an oxalate of mercury.

Dependence of Film Formation on Carbon Dioxide Pressure

The object of this experiment is to determine the wall dependence of product formation. High carbon dioxide pressures at relatively high mercury pressures (corresponding to room temperature droplets) will inhibit diffusion to the wall of solid products, if formed away from the wall. The relative rate of product formation can be monitored via the carbon monoxide analysis.

Experimental: The reactor is described in Figure 25. No DMA filter was used in all cases. The lithium fluoride window was Co^{60} γ-irradiated and served as a filter (29). The reactor was filled and analyzed on an auxillary outlet of the storage manifold of the vacuum system (see Figure 17). The conditions and results of the four reactions performed in this experiment are listed in Table XIII.

Conclusions: The retarded yield rate at lower carbon dioxide pressure was due to film formation on the window (1849A absorption). The film was not formed on the window at the higher carbon dioxide pressures because the path to the window of the solid products was obstructed by carbon dioxide molecules, allowing profusion throughout the reactor.

FIGURE 25

REACTOR WITH REMOVABLE WINDOW

Legend:

A Removable window, silica or lithium fluoride

B Ground joint, S 18/9

C Vacuum stopcock

D Pyrex body

REACTOR WITH REMOVABLE WINDOW

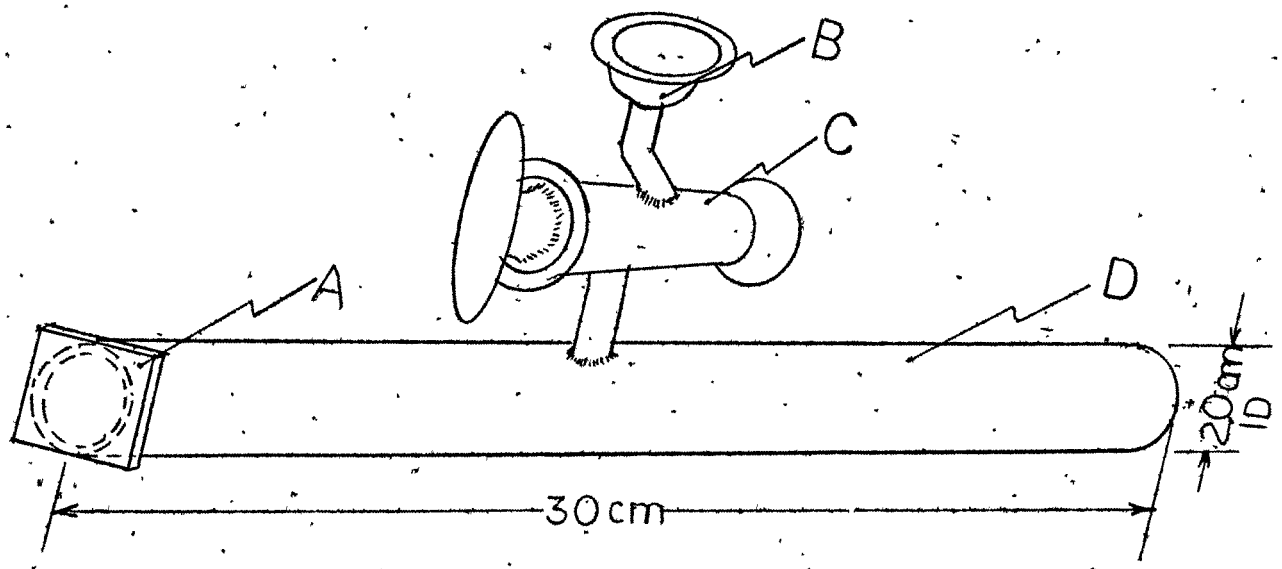

TABLE XIII

DATA OF FILM-CO_2 PRESSURE RELATION EXPERIMENT

Run	A	B	C	D
Window	LiF	SiO_2, foil mask	SiO_2	bleached LiF, foil mask
Pressure Reactant CO_2	252.8 torr	244.5 torr	21.5 torr	22.2 torr
Run Time	11 hours	11.3 hours	5 hours	5 hours
Yield CO(g) per hour		0.0406 torr/ hour	0.0237 torr/ hour	0.0273 torr/ hour

Appearance of Film:

RUN A: Noticed bleaching of windownand tiny mercury droplets on window, but no yellow film. A ring of yellow and silvery white products formed 142 millimeters from the windowa The ring was 15 mm wide.

RUN B: No noticeable film on window, no ring as in Run A.

RUN C: Yellow film appeared only on window in the exact shape of the mask opening.

RUN D: Yellow film appeared only on window with the exact shape of the mask opening.

Discussion

Summary of Results

The results of the Hg6 $^1P_1$ photosensitized decomposition of carbon dioxide described in Section III can now be summarized. The products of the reaction are carbon monoxide, mercuric oxide, and mercuric oxalate. No atomic oxygen is formed. The rates of product formation are linearly dependent on the intensity of the 1849A radiation.

The rates of production of carbon monoxide and oxalate have the same dependence on carbon dioxide pressure. The rates of product formation are not a function of mercury vapor concentration (providing the mercury vapor pressure concentration can be maintained constant), and neither are they wall dependent.

The rate of product formation is suppressed by light absorption from the film formation. The mercuric oxalate product is consequently decomposed to yield the reactants, carbon dioxide and mercury.

The results indicate the following mechanism

$$Hg(6\,^1S_o) + h\nu(1849) \xrightarrow{I_o} Hg(6\,^1P_1) \qquad (1)$$

$$Hg(6\,^1P_1) \xrightarrow{1/\tau} Hg(6\,^1S_o) + h\nu(1849) \qquad (2)$$

$$Hg(6\,^1P_1) + CO_2 \xrightarrow{k_1} HgOCO^* \qquad (3)$$

$$HgOCO^* \xrightarrow{k_2} HgO(s) + CO \qquad (4)$$

$$HgOCO^* \xrightarrow{k_3} HgOCO^3 + \text{heat} \qquad (5)$$

$$HgOCO^* \xrightarrow{k_4} Hg + CO_2 \qquad (6)$$

$$HgOCO^3 + CO_2 \xrightarrow{k_5} HgC_2O_4(s) \qquad (7)$$

$$HgC_2O_4 + h\nu \xrightarrow{I_o, I_{uv}} Hg + CO \qquad (8)$$

where I_o = incident intensity of reversible 1849A radiation

I_{uv} = incident intensity of other ultraviolet radiation

τ = lifetime of Hg6 $^1P_1$ atoms

HgOCO* = excited (singlet) complex

$HgOCO^3$ = excited, but metastable, triplet complex

k_i = rate constant of step i.

This mechanism predicts the rates of product appearance, involving Hg6 $^1P_1$, HgOCO*, and $HgOCO^3$, according to the following relationships:

$$\frac{d(CO)}{dt} = \frac{d(HgO)}{dt} = \left[\frac{k_2}{k_2+k_3+k_4} \cdot \frac{I_o(CO_2)}{\frac{1}{k_1\tau} + (CO_2)} \right] T_{1849}\, T'_{1849} \qquad (9)$$

$$\frac{d(HgC_2O_4)}{dt} = \frac{k_3}{k_2+k_3+k_4} \cdot \frac{I(CO_2)}{\frac{1}{k_1\tau} + (CO_2)} - \sum_{\lambda=1849A}^{\approx 4000A} I_{o\lambda} T'_\lambda (1-T_\lambda) \qquad (10)$$

where $I_{o\lambda}$ = intensity of radiation emerging from reactor innerwall at wavelength λ

T_λ = transmittance of HgC_2O_4 component of film at wavelength λ

T_λ' = transmittance of HgO component of film at wavelength λ

Although the conditions in the reactor were slowly changing due to the attenuation of incident radiation by the film formation, it is assumed that the change was very slow compared to the ability of the steady state concentration to follow the gradual change in I_o, and

therefore of negligible concern in the qualitative interpretation of the data. Also, it was shown that in the case of the multiple reactor system the attenuation of rate did not become apparent until after about 25 minutes reaction time (see Figure 15). The same conditions probably apply to the data taken with the single reactor system at low mercury pressures, since the product yield was also quite low.

The Nature of the HgOCO Intermediate

It is seen that the postulate of the HgOCO* species readily explains the absence of atomic and molecular oxygen formation. The decay to metastable $HgOCO^3$ and subsequent reaction with CO_2 to form oxalate is in accord with the parallel dependence of carbon monoxide and mercuric oxalate production on I_o, carbon dioxide pressure, and time. The fact that the ratio of carbon monoxide to oxalate products is variable is due to the photolysis of the mercuric oxalate which varies from run to run according to the variation in lamp spectra.

The singlet to triplet transition in the complex must be very fast, in fact, competitive with the destructive decay of the singlet and with the rate of carbon dioxide collisions with HgOCO*, which can be estimated. In order to withstand the carbon dioxide pressures in the reactor, the (excited) complex formed must have certain properties. The carbon dioxide pressure, that is, collisions of carbon dioxide molecules with the complex, may very likely cause disturbances in the reaction coordinates. These disturbances may be induced dissociation, oxalate formation, or deactivation. The collision may

thereby cause a complex dependence on carbon dioxide pressure of the yield, which is not evident in the carbon monoxide or mercuric oxalate rate dependence in the plateau regions of carbon dioxide pressure dependence. Thus all transformation processes must take place within the time of one collision at the highest pressure studied (200 torr). If the collision diameter is assumed to be the sum of the diameter of carbon dioxide and mercury molecules, the collision frequency of a complex molecule with carbon dioxide would be approximately 1.8×10^{10} per second. If it is assumed that the results can begin to discern a 10% change in yield due to CO_2 pressure (see Figure 14), a time interval of 5×10^{-12} seconds is provided the complex to conduct itself through its product forming processes. If a collision efficiency of 10% for the perturbation of these processes by carbon dioxide collisions is allowed, which is reasonable, considering the poor efficiency of carbon dioxide to undergo collisionally induced vibrational changes (47), then the time interval may be expanded to 5×10^{-11} seconds. Thus the decomposition process,

$$HgOCO^* \rightarrow HgO + CO$$

and the transition to the triplet

$$HgOCO^* \rightarrow HgOCO^3$$

must each take place within 5×10^{-11} seconds.

This time interval would correspond to approximately two hundred vibrations in the bond corresponding to the reaction coordinate, at a

frequency that is determined by

$$\nu = - \frac{kT}{h}$$

where ν = vibration frequency of reaction coordinate

k = Boltzmann's constant

T = room temperature, absolute

h = Planck's constant

A plausible scheme for the dual fate of the complex may be visualized in terms of the energy diagram of the complex (see Figure 26). The complex is formed in a singlet antibonding electronic state. This state is also close to or at the point of intersystem crossing to the triplet. The ratio of the probability of the decomposition of the singlet to that crossing to the triplet can be close to unity if the perturbations in the triplet and singlet molecular orbitals are great enough (strict singlet to triplet crossing is forbidden)(48).

The perturbations in the states of the complex include the magnetic interaction with the very large mercury nucleus (49) and the allowedness of several modes of complex formation. Some of these

FIGURE 26

POSSIBLE ENERGY DIAGRAM OF EXCITED SINGLET COMPLEX

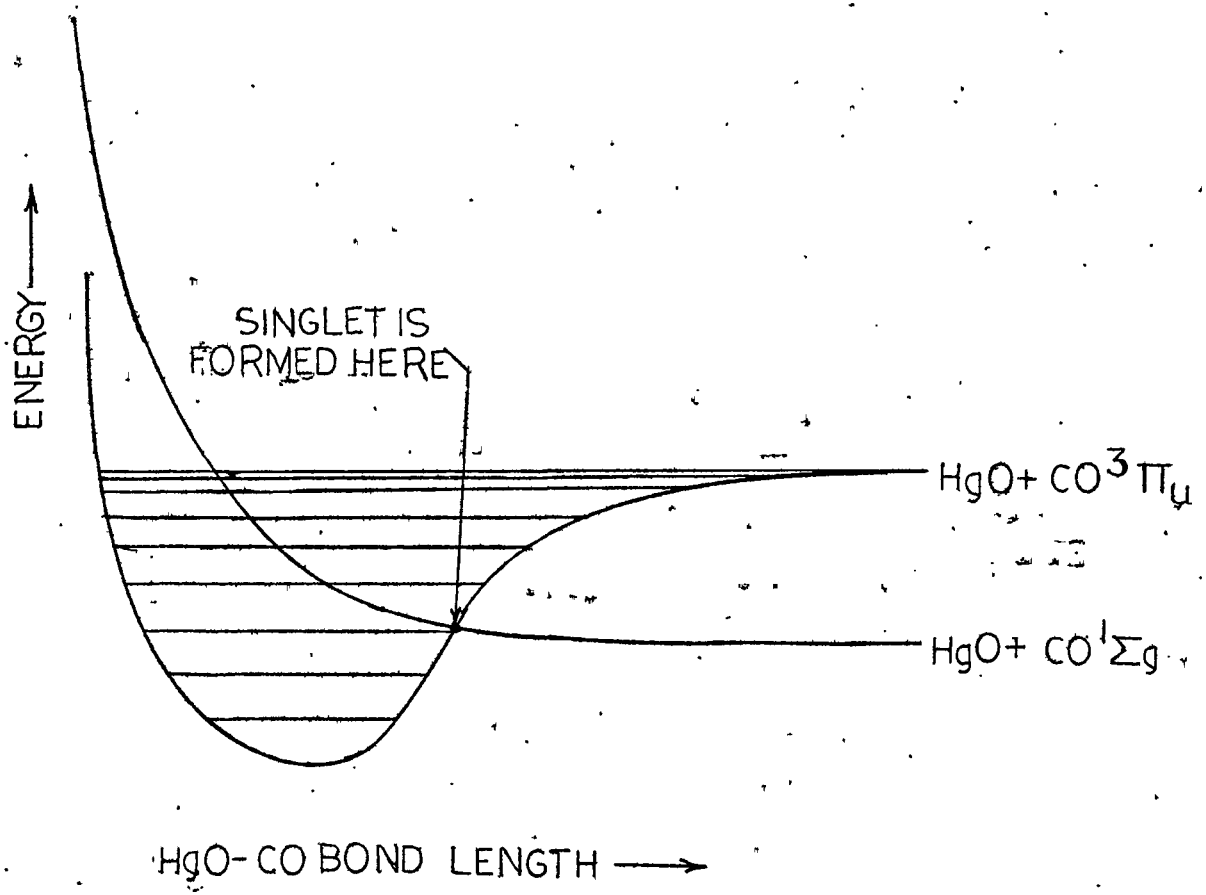

modes may be the following:

a) p-π molecular orbital; one of the π_g^4 electrons of the carbon dioxide molecule further delocalizes to include the vacant 6 p orbital of the mercury atom.

b) charge transfer to the carbon dioxide molecule from the Hg6 $^1P_1$ orbital; the ionization potential of the mercury atoms is now in the alkali range, however, the electron affinity of carbon dioxide is not known.

c) charge transfer <u>from</u> the carbon dioxide molecule to the vacant Hg6 ^1S_o orbital; the electron affinity of mercury, Hg6 $^1P_1$ in this case, would possibly be quite large due to decreased screening of the nucleus and the lower energy level of the entering electron, however, the ionization potential of carbon dioxide from π_g^4 orbital is approximately 13 ev (19), but that for a non-bonding oxygen electron may be less.

Although these modes express possible mechanisms of spontaneous reaction of the excited complex, there is no proof that any of them is the mechanism. Temperature dependence (activation energy) studies and fluorescence and phosphorescence studies of this region could help to elucidate the exact reaction coordinates and the energetic characteristics of product formation from the complex.

<u>Quenching Cross Section Determination</u>

A calculation of the cross section of carbon dioxide for the quenching of the energy (6.7 ev) of Hg6 $^1P_1$ atoms has been made of each of the three sets of CO_2 pressure-product relationship data. They are listed in Table XIV.

TABLE XIV

QUENCHING CROSS SECTION CALCULATIONS

System	Mercury Droplet Temperature	KNl	(τ= 0.3x10^{-9}sec) σ^2	(τ=1.6 x 10^{-9}sec) σ^2
Single Reactor	-33°C	56	4690A^2	875A^2
Single Reactor	22°C	2500	7210A^2	1350A^2
Multiple Reactor	22°C	1800	32800A^2	6130A^2

These values appear not only in disagreement with each other but also as absurdly high in quantity. The large values are due to the fact that imprisonment of the 1849A resonance radiation occurs in the reactor (1). The resonance radiation re-emitted by natural decay of Hg6 $^1P_1$ atoms in the reactor is reabsorbed by Hg6 ^1S_o atoms, which are in much larger proportion in the reactor. Should they exist as Hg6 $^1P_1$ for the mean lifetime of Hg6 $^1P_1$ without being quenched by carbon dioxide, they will re-emit, and their corresponding irradiation will again cause the same sequence, until the irradiation is completely consumed by quenching of Hg6 $^1P_1$ atoms (Lorentz broadening) and loss through the boundaries of the reactor. This diffusion of the resonance radiation has been treated theoretically (1) for the simplest of experimental conditions, and even then is the calculation of quenching cross sections very complex. Qualitatively, this treatment

shows that the apparent quenching cross section is very heavily dependent on the value KNl, which is the negative of the natural logarithm of the transmission of the "reversible" 1849A radiation by the mercury in the cell, and is called equivalent opacity (1). This dependence reflects the fact that the greater KNl, the greater the number of diffusing processes will be. The quenching cross section must be determined for a number of equivalent opacities, preferably no greater than kNl = 3, and extrapolated to KNl = 0, which corresponds to the true cross section value. As can be seen, the KNl values of this research are nowhere near this range, and furthermore, the problem of the virtual leak of adsorbed mercury atoms would strenuously prohibit any attempt to approach KNl = 0 to 3 for Hg6 $^1P_1$ resonance. The kNl calculated to correspond to a mercury liquid temperature of -33°C was two, however, the value of 56 in Table XIV reflects the mercury liquid temperature corresponding to the actual mercury vapor concentration as determined by the mercury vapor dependence runs. The value of K is approximate, being that derived by Garrett (50) in his experiments. It is very likely that the quenching cross section values obtained by Mori (8) are also too large, and require a similar treatment.

The values of quenching cross section for the single and multiple reactor systems at 22°C do not agree well because the heavier film formation in the single reactor system, due to its retardation of the reaction rate, gives erratic pressure dependence curves which must be extrapolated as a function of time to correspond to the condition at which the film's 1849A absorption is negligible, as was shown to be the case in the multiple reactor runs (Figure 14).

IV.

CONCLUSION

CONCLUSIONS

A system for studying the photosensitization reactions of Hg6 $^1P_1$ atoms was developed. This system relies on a deoxygenated cyclohexane solution of 9,10 dimethyl anthracene as a filter for the removal of 2537A radiation from the resonance lamp, which would otherwise allow Hg6 $^3P_1$ atoms to be formed in the reactor and consequently confuse the interpretation of the results.

The photosensitized decomposition of carbon dioxide with mercury 6 $^1P_1$ atoms was performed using this system. The products of the reaction were mercuric oxide, carbon monoxide, and mercuric oxalate. The mercuric oxalate is subject to decomposition by ultraviolet light, and without the filter, which removed the predominant but undesirable 2537A radiation, would never have appeared. This product has never been reported in other similar studies. The mercuric oxide was shown to have formed directly, that is, it was not formed by the combination of oxygen atoms from the dissociation of an excited carbon dioxide molecule and mercury atoms. The rates of carbon monoxide production and mercuric oxalate production have the same carbon dioxide pressure, mercury pressure, and time dependence. The solid products (mercuric oxalate and mercuric oxide) were shown to form a film on the reactor only at low substrate pressures, and it was shown that the formation of the film was not necessary for the formation of the products and thus the reaction is not wall dependent.

From these phenomena it is concluded that the reaction of carbon dioxide with mercury $6\,{}^1P_1$ atoms most likely results in the formation of an excited (singlet) complex, HgOCO*, which decomposes directly to yield mercuric oxide and carbon monoxide and which also undergoes a competitive transition to a triplet metastable state. The metastable state may then react with carbon dioxide to form mercuric oxalate.

BIBLIOGRAPHY

1. Mitchell, A. C. G. and M. W. Zemansky, Resonance Radiation and Excited Atoms (Cambridge University Press, 1961).

2. Chapman, D. L., Chadwick, S. and J. E. Ramsbottom, J. Chem. Soc. 91, 951 (1907).

3. E. Herschfinkel, Comp. rend. 149, 395 (1909).

4. H. Tramm, Z. physik. Chem. 105, 356 (1923).

5. Coehn, A., and B. W. May, Z. physikal. Chem. B26, 117 (1934).

6. Cline, J. E. and G. S. Forbes, J. Am. Chem. Soc. 61, 716 (1939).

7. Strausz, O. P. and H. E. Gunning, Can. J. Chem. 39, 2244 (1961).

8. Y. Mori, Bull. Chem. Soc. Japan, 34, 1128 (1961).

9. M. H. J. Wijnen, J. Chem. Phys., 24, 851 (1956).

10. McGilvery, J. D. and C.A. Winkler, Can. J. Chem. 30, 194 (1952).

11. Drechsel, Ann. 146, 140 (1868).

12. Lemarchands, M. and H. L. Roman, Compt. rend. 192, 1381 (1931).

13. Wolff, C. M. and R. Pertel, J. Phys. Chem. 69, 4047 (1965).

14. Wagman, D. D., Kilpatrick, J. E., Taylor, W. J., Pitzer, K. S. and F. D. Rossini, J. Res. Nat. Bur. Stand. 34, 143 (1945).

15. Wagman, D. D., Kilpatrick, J. E., Taylor, W. J., Pitzer, K. S., and F. D. Rossini, J. Res. Nat. Bur. Stand. 34, 143 (1945).

16. Cottrell, T. L., The Strength of Chemical Bonds, 2nd ed. (London: Butterworths, 1958), p. 200.

17. Cottrell, ibid., 155.

18. Cottrell, ibid., 161.

19. R. S. Mulliken, Can. J. Chem. 36, 10 (1958).

20. S. W. Leifson, Astrophys. J., 63, 73 (1926).

21. G. Herzberg, Molecular Spectra and Molecular Structure, Vol. III. (Princeton: Van Nostrand, 1966), p. 500.

22. Herzberg, ibid., 430.

23. K. Kraus, Z. fur Naturf. 16a, 1381 (1961).

24. Craggs, J. D., and B. A. Tozer, Proc. Roy. Soc. London, 254A, 229 (1960).

25. N. A. Supplice, Brit. J. Appl. Phys. 12, 214 (1961).

26. M. Matsui, Sci. Papers Inst. Phys. Chem. Research 53, 290 (1959).

27. A. Póitier, J. chim. phys. 50, 10 (1953).

28. R. S. Mulliken, presented at 11th Annual Welch Conference, Houston, December 1967.

29. Weeks, J. L., Gordon, S., and G. M. A. C. Meaburn, Nature 191, 1186 (1961).

30. W. Baumeister, Properties of Multilayer Filters, NASA Accession Number N66-37582 Category 23 (1966).

31. Jones, L. C., Jr. and L. W. Taylor, Anal. Chem. 27, 228 (1955).

32. Friedel, R. A. and M. Orchin, Ultraviolet Spectra of Organic Compounds (New York: Wiley, 1951), p. 388.

33. R. Livingstone, Photochemistry in the Liquid and Solid States (New York: Wiley, 1960), p. 76.

34. A. Willemart, Comp. rend. 205, 993 (1937).

35. Wolff, C. M. and R. Pertel, J. Opt. Soc. Am. 54, 1168 (1964).

36. Johnson, F. S., Watanabe, K. and R. Tousey, J. Opt. Soc. Am. 41, 702 (1951).

37. N. V. Sidgwick, Chemical Elements and their Compounds (London: Oxford, 1950), p. 319.

38. F. Feigl, Spot Tests in Organic Analysis, 5th ed. (New York: Elsevier, 1956), p. 355.

39. F. Daniels, J. H. Mathews, J. W. Williams, P. Bender, and R. A. Alberty, Experimental Physical Chemistry, 5th ed. (New York: McGraw-Hill, 1956), p. 243.

40. C. D. Hodgman, ed., Handbook of Chemistry and Physics, 44th ed. (Chemical Rubber; Cleveland, 1963), p. 2647.

41. N. L. Ruland, Doctoral Thesis, University of Houston, 1967.

42. Melville, H. and B. G. Gowenlock, Experimental Methods in Gas Reactions (New York: MacMillan, 1964), p. 64.

43. Honig, R. E., and H. O. Hook, RCA Rev. 21, 360 (1960).

44. Smith, A. N., Swinehart, J. and E. D. Lesnini, Anal. Chem. 30, 1217 (1958).

45. Dal Nogare, S. and R. S. Juvet, Jr., Gas-Liquid Chromatography (New York: Interscience, 1962), p. 388.

46. Dal Nogare and R. S. Juvet, ibid, p. 391.

47. I. M. Metter, J. Exptl. Theoret. Phys. (U.S.S.R.) 8, 734 (1938).

48. N. J. Turro, Molecular Photochemistry (Benjamin: New York, 1966), p. 75.

49. Turro, ibid., p. 50.

50. Garrett, P. H., Phys. Rev. 40, 779 (1932).